remains unknown whether *EGFR* mutation in cancer is correlated with clinical response to EGFR-specific tyrosine kinase inhibitors (EGFR-TKI). *EGFR* mutation in other types of tumors than lung cancer seems correlated with immunohistochemical expression but correlation with gene amplification is unknown [14]. Functional aspects of *EGFR* mutation in other types of tumors are also only partially understood. To clarify the significance of somatic mutations in various tumors, tissue banking is necessary. In addition, validated and standardized analytical methods and cross-validation are important to give consistent results. We should also consider how to conduct clinical trials of target-based drugs for less common tumors based on biological data.

Ethnic difference in *EGFR* mutation

Ethnic difference in *EGFR* mutation is another important topic. It is considered that ethnic differences may determine both the frequency of *EGFR* mutation and response to TKi [2]. However, although it has not been fully discussed whether these differences are due to ethnic or merely geographical divides, ethnicity can explain differences in clinical response because of the data acquired in Asian–US patients. It is also considered that differences among the regions of Asia might be obtained: patterns of *EGFR* mutation may differ between Japanese, Chinese, Korean, South Indian, and Turkish individuals [16]. Expanding genome databases should eventually pinpoint the contribution of ethnicity in this regard. Already there is some evidence related to ethnic differences. A CA repeat exists in exon 1 of *EGFR*, related to transcriptional level of this gene. The length of CA repeat varies and is related to ethnicity [9]. Japanese have longer CA repeat compared with Caucasians. Moreover, intron 1 polymorphism reportedly mediates response to EGFR-TKI [1].

What are the differences among the types of *EGFR* mutation? The deletion mutation in exon 19 and point mutation L858R in exon 21 are the two major mutations. Previously, we speculated that the deletion mutation is more frequently detected in Japanese and Asian lung cancer patients as compared with Caucasians. However, recent data seem to refute ethnic difference in the types of *EGFR* mutations [12].

A predictive biomarker related to ethnic difference of sensitivity to gefitinib

Ethnic difference might also exist in sensitivity to drugs. In most such cases, gene polymorphism including microsatellite polymorphism and single nucleotide polymorphism may explain ethnic difference of response to drugs.

Using microarray technique, we analyzed gene expression profiles of peripheral mononuclear cells in lung cancer patients receiving gefitinib as a first-line monotherapy. Our results revealed that HLA genotype was closely related to response to this agent. On the other hand, large ethnic difference of HLA genotype was recognized. Previous reports have demonstrated that HLA genotype plays a role in the metabolism of certain drugs and may be a prognostic factor in malignancies such as gastric, ovarian, and cervical cancers [6, 11, 13, 15, 17]. We hypothesize that HLA subtype may be related to response to gefitinib and might explain ethnic differences. Cross-validation study of this HLA biomarker is ongoing.

Ethnic difference of gefitinib toxicity profile

Subpopulation analysis of gefitinib's toxicity in the ISEL study revealed that only southwest Asian and Taiwanese patients exhibited high ratios of interstitial lung disease (ILD) while on this therapy [16]. However, ILD might not have been induced by gefitinib. More interestingly, the data indicated that Indian–British patients experienced severe (grade 3) skin toxicity along with higher response to gefitinib. Although these phenomena are based on subpopulation analysis, we can speculate that ethnic difference might guide toxicity as well as clinical response to EGFR-TKI. Genomic and biomarker research is necessary to further elucidate these preliminary findings.

Acknowledgment We thank Dr. N. Thatcher (Christie Hosp NHS Trust) for personal communication with T. Kato.

References

1. Amador ML, Oppenheimer D, Perea S, Maitra A, Cusati G, Iacobuzio-Donahue C, Baker SD, Ashfaq R, Takimoto C, Forastiere A, Hidalgo M (2004) An epidermal growth factor receptor intron 1 polymorphism mediates response to epidermal growth factor receptor inhibitors. Cancer Res 64:9139–9143
2. Calvo E, Baselga J (2006) Ethnic differences in response to epidermal growth factor receptor tyrosine kinase inhibitors. J Clin Oncol 24:2158–2163
3. Cohen EE, Lingen MW, Martin LE, Harris PL, Brannigan BW, Haserlat SM, Okimoto RA, Sgroi DC, Dahiya S, Muir B, Clark JR, Rocco JW, Vokes EE, Haber DA, Bell DW (2005) Response of some head and neck cancers to epidermal growth factor receptor tyrosine kinase inhibitors may be linked to mutation of *ERBB2* rather than *EGFR*. Clin Cancer Res 11:8105–8108

4. Douglas DA, Zhong H, Ro JY, Oddoux C, Berger AD, Pincus MR, Satagopan JM, Gerald WL, Scher HI, Lee P, Osman I (2006) Novel mutations of epidermal growth factor receptor in localized prostate cancer. Front Biosci 11:2518–2525
5. Gwak GY, Yoon JH, Shin CM, Ahn YJ, Chung JK, Kim YA, Kim TY, Lee HS (2005) Detection of response-predicting mutations in the kinase domain of the epidermal growth factor receptor gene in cholangiocarcinomas. J Cancer Res Clin Oncol 131:649–652
6. Klein B, Klein T, Nyska A, Shapira J, Figer A, Schwartz A, Rakovsky E, Livni E, Lurie H (1991) Expression of HLA class I and class II in gastric carcinoma in relation to pathologic stage. Tumour Biol 12:68–74
7. Lee JW, Soung YH, Kim SY, Nam HK, Park WS, Nam SW, Kim MS, Sun DI, Lee YS, Jang JJ, Lee JY, Yoo NJ, Lee SH (2005) Somatic mutations of *EGFR* gene in squamous cell carcinoma of the head and neck. Clin Cancer Res 11:2879–2882
8. Lee SC, Lim SG, Soo R, Hsieh WS, Guo JY, Putti T, Tao Q, Soong R, Goh BC (2006) Lack of somatic mutations in *EGFR* tyrosine kinase domain in hepatocellular and nasopharyngeal carcinoma. Pharmacogenet Genomics 16:73–74
9. Liu W, Innocenti F, Chen P, Das S, Cook EH Jr, Ratain MJ (2003) Interethnic difference in the allelic distribution of human epidermal growth factor receptor intron 1 polymorphism. Clin Cancer Res 9:1009–1012
10. Lynch TJ, Bell DW, Sordella R, Gurubhagavatula S, Okimoto RA, Brannigan BW, Harris PL, Haserlat SM, Supko JG, Haluska FG, Louis DN, Christiani DC, Settleman J, Haber DA (2004) Activating mutations in the epidermal growth factor receptor underlying responsiveness of non-small-cell lung cancer to gefitinib. N Engl J Med 350:2129–2139
11. Ogoshi K, Tajima T, Mitomi T, Makuuchi H, Tsuji K (1997) HLA-A2 antigen status predicts metastasis and response to immunotherapy in gastric cancer. Cancer Immunol Immunother 45:53–59
12. Riely GJ, Pao W, Pham D, Li AR, Rizvi N, Venkatraman ES, Zakowski MF, Kris MG, Ladanyi M, Miller VA (2006) Clinical course of patients with non-small cell lung cancer and epidermal growth factor receptor exon 19 and exon 21 mutations treated with gefitinib or erlotinib. Clin Cancer Res 12:839–844
13. Ryu KS, Lee YS, Kim BK, Park YG, Kim YW, Hur SY, Kim TE, Kim IK, Kim JW (2001) Alterations of HLA class I and II antigen expression in preinvasive, invasive and metastatic cervical cancers. Exp Mol Med 33:136–144
14. Schilder RJ, Sill MW, Chen X, Darcy KM, Decesare SL, Lewandowski G, Lee RB, Arciero CA, Wu H, Godwin AK (2005) Phase II study of gefitinib in patients with relapsed or persistent ovarian or primary peritoneal carcinoma and evaluation of epidermal growth factor receptor mutations and immunohistochemical expression: a gynecologic oncology group study. Clin Cancer Res 11:5539–5548
15. Shen YQ, Zhang JQ, Miao FQ, Zhang JM, Jiang Q, Chen H, Shan XN, Xie W (2005) Relationship between the downregulation of HLA class I antigen and clinicopathological significance in gastric cancer. World J Gastroenterol 11:3628–3631
16. Thatcher N, Chang A, Parikh P, Rodrigues Pereira J, Ciuleanu T, von Pawel J, Thongprasert S, Tan EH, Pemberton K, Archer V, Carroll K (2005) Gefitinib plus best supportive care in previously treated patients with refractory advanced non–small-cell lung cancer: results from a randomised, placebo-controlled, multicentre study (Iressa survival evaluation in lung cancer). Lancet 366:1527–1537
17. Vitale M, Pelusi G, Taroni B, Gobbi G, Micheloni C, Rezzani R, Donato F, Wang X, Ferrone S (2005) HLA class I antigen down-regulation in primary ovary carcinoma lesions: association with disease stage. Clin Cancer Res 11:67–72

Research Article

A Photon Counting Technique for Quantitatively Evaluating Progression of Peritoneal Tumor Dissemination

Kazuyoshi Yanagihara,[1] Misato Takigahira,[1] Fumitaka Takeshita,[2] Teruo Komatsu,[1] Kazuto Nishio,[3] Fumio Hasegawa,[4] and Takahiro Ochiya[2]

[1]Central Animal Laboratory, [2]Section for Studies on Metastasis, [3]Pharmacology Division, and [4]Central RI Laboratory, National Cancer Center Research Institute, Tokyo, Japan

Abstract

We recently established a mouse model of peritoneal dissemination of human gastric carcinoma, including the formation of ascites, by orthotopic transplantation of cultured gastric carcinoma cells. To clarify the processes of expansion of the tumors in this model, nude mice were sacrificed and autopsied at different points of time after the orthotopic transplantation of the cancer cells for macroscopic and histopathologic examination of the tumors. The cancer cells grew actively in the gastric submucosa and invaded the deeper layers to reach the serosal plane. The tumor cells then underwent exfoliation and became free followed by the formation of metastatic lesions initially in the greater omentum and subsequent colonization and proliferation of the tumors on the peritoneum. Although this model allowed the detection of even minute metastases, it was not satisfactory from the viewpoint of quantitative and objective evaluation. To resolve these problems, we introduced a luciferase gene into this tumor cell line with a high metastasizing potential and carried out *in vivo* photon counting analysis. This photon counting technique was found to allow objective and quantitative evaluation of the progression of peritoneal dissemination on a real-time basis. This animal metastatic model is useful for monitoring the responses of tumors to anticancer agents. (Cancer Res 2006; 66(15): 7532-9)

Introduction

Tumor dissemination and ascites are the two major features of cancerous peritonitis. Of the various manifestations of the progression of cancer affecting the i.p. organs (gastric, hepatic, ovarian, and other cancers), cancerous peritonitis is the most closely associated with poor operative results (1–6). In particular, scirrhous gastric cancer (diffusely infiltrative carcinoma or Borrmann's type IV carcinoma or the linitis plastica type) is a high-grade gastric cancer that is difficult to detect in the early stages and is often complicated by peritoneal dissemination (7–9). Although peritoneal dissemination is an important subject, very few experimental studies have been conducted to characterize its occurrence. In general, most of the experimental models of peritoneal dissemination from gastric cancer established to date have involved direct i.p. implantation of cancer cells (10–12). Although these conventional models may allow limited examination of the later stages of peritoneal dissemination, they cannot be expected to allow reasonable evaluation of its early stages. It is well known that implanting human tumor fragments and tumor cells orthotopically into the corresponding organs of nude mice results in much higher metastatic rates (13, 14). However, only one orthotopic implantation model, scirrhous carcinoma of the stomach, has been reported (15). We recently established two scirrhous gastric carcinoma-derived tumor cell lines capable of spontaneous metastasis following ectopic implantation (16). We repeated cycles of orthotopic transplantation of these tumor cell lines, collected cancer cells from the ascitic fluid formed as a result of cancerous peritonitis, and used the collected cells for further cycles of orthotopic transplantation. In this way, we isolated cell lines (44As3, 58As1, and 58As9) with high metastasizing potential and stable metastatic characteristics (17). When these cells were implanted orthotopically into the animals, bloody ascites formed within 3 to 5 weeks, resulting in the death of the animals.

As stated above, conventionally, progression of peritoneal dissemination has been analyzed by implanting cancer cells directly into the peritoneal cavity followed by sacrifice and autopsy of the animals at certain points of time after implantation and, finally, measurement of the number and weight of the tumor nodules in the sacrificed animals (18–20). Evaluation of the efficacy of anticancer agents was also hampered by this limitation (21–25). Evaluation using these methods may be affected by subjective factors and, therefore, unsatisfactory from the viewpoint of quantitative or objective evaluation. In order for our animal model of peritoneal dissemination to be applied universally as a drug evaluation system, we needed to establish a method for quantitative observation and objective evaluation of the relevant variables.

Recent progress in the optical imaging of cancers in animal models presents many potential advantages for recreating the disease process, disease detection, screening, diagnosis, drug development, and treatment evaluation. Fluorescence-based imaging (26–35) and photon counting analysis (36–43) modalities are well developed and allow specific, highly sensitive and quantitative measurements of a wide range of tumor-related variables in mice. Herein, we have shown that photon counting technique is an effective technology in living mice.

Materials and Methods

Established highly metastatic cell lines and culture. 44As3, highly peritoneal metastatic cell line, and parent HSC-44PE, human scirrhous gastric carcinoma-derived cell line, were previously reported (16, 17). When the subclones isolated by repeated s.c. injection of HSC-44PE cells were implanted orthotopically, they spread to the greater omentum, mesenterium, etc. and caused the formation of bloody ascites in a few animals (16). We repeated cycles of isolation of ascitic tumor cells and orthotopic inoculation of these cells, in turn, into animals to isolate highly metastatic

Requests for reprints: Kazuyoshi Yanagihara, Central Animal Laboratory, National Cancer Center Research Institute, 5-1-1 Tsukiji, Chuo-ku, Tokyo 104-0045, Japan. Phone: 81-3-3542-2548; Fax: 81-3-3542-2548; E-mail: kyanagih@gan2.res.ncc.go.jp.

doi:10.1158/0008-5472.CAN-05-3259

44As3 cell lines, having a strong capability of inducing the formation of ascites (17).

The cell lines were maintained in RPMI 1640 supplemented with 10% FCS (Sigma Chemical, St. Louis, MO), 100 IU/mL penicillin G sodium, and 100 mg/mL streptomycin sulfate (Immuno-Biological Laboratories, Takasaki, Japan) in a 5% CO_2 and 95% air atmosphere at 37°C (17).

***In vivo* photon counting analysis.** 44As3 and HSC-44PE cells were transfected with a complex of 4 μg pEGF-PLuc plasmid DNA (Clontech, Palo Alto, CA) and 24 μL GeneJammer reagent (Stratagene, Cloning Systems, La Jolla, CA) in accordance with the manufacturer's instructions. Stable transfectants were selected in geneticin (400 μg/mL; Invitrogen, Carlsbad, CA), and bioluminescence was used to screen transfected clones for luciferase gene expression using the IVIS system (Xenogen, Alameda, CA). Clones expressing the luciferase gene were named 44As3Luc and HSC44Luc.

Orthotopic implantation of 1×10^6 44As3Luc and HSC44Luc cells was conducted in 6-week-old female BALB/c-*nu/nu* mice (day 0) as described previously (17). *In vivo* photon counting analysis was conducted on a cryogenically cooled IVIS system using Living Image acquisition and analysis software (Xenogen) as described previously (39).

Animal protocols were approved by the committee for Ethics of Animal Experimentation and were in accordance with the Guideline for Animal Experiments in the National Cancer Center. Mice were purchased from CLEA Japan (Tokyo, Japan). The mice were maintained under specific pathogen-free conditions and provided with sterile food, water, and cages. Ambient light was controlled to provide regular cycles of 12 hours of light and 12 hours of darkness.

Therapeutic study with irinotecan (CPT-11). The experimental mice were divided into a control group that received vehicle alone (saline) and experimental groups that received i.v. inoculation of 200 mg/kg/mouse of CPT-11, a clinically active topoisomerase I inhibitor, a level that has been reported to be highly effective in tumor growth (17). On days 3, 7, and 11, tumor-bearing mice received an i.v. injection of CPT-11. The additional injection of CPT-11 was done on days 28, 31, and 35. CPT-11 was purchased from Yakult Honsha (Tokyo, Japan) and dissolved in saline before being injected.

Statistical analysis. All data were analyzed by using the unpaired t test and expressed as the mean ± SE. A $P < 0.05$ was considered statistically significant.

Results

Animal model of peritoneal dissemination. The highly metastatic peritoneal cell line used in this study (44As3) was isolated by repeated cycles of orthotopic implantation of HSC-44PE cells and collection of the ascitic tumor cells as described in Materials and Methods (16, 17). As shown in Table 1 and Fig. 1, the tumor formed by this cell line was characterized by a propensity for early peritoneal dissemination and was frequently associated with the formation of ascites and the animals became moribund ~35 days after implantation. On the other hand, the graft cell survival after implantation of the parent cell line (HSC-44PE) was 67% and moribund animals were not seen until ~90 days after implantation, although no ascites formation was observed.

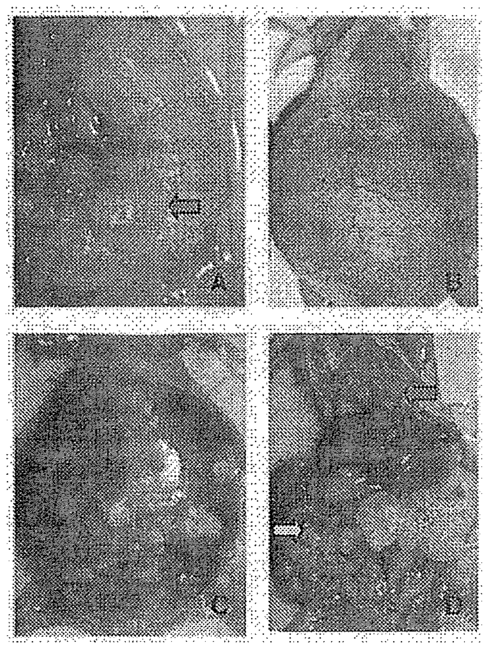

Figure 1. Macroscopic appearance of the peritoneal disseminations after orthotopic implantation of 44As3 cells. *A, green arrow,* orthotopic implantation of the cells in the stomach of nude mice was followed by tumor formation 3 weeks later. *B* and *C,* carcinomatous peritonitis was observed 5 weeks after orthotopic implantation of the cells. Abdominal distension because of bloody ascites was evident. *D,* peritoneal dissemination was recognized from the innumerable whitish nodules visualized in the abdominal cavity, mesenterium (*yellow arrow*), omentum, parietal peritoneum, and diaphragm (*green arrow*).

Anatomic, histopathologic, and ultrastructural analysis of the progression of peritoneal dissemination. To analyze the process of progression of peritoneal dissemination, 44As3 cells (1×10^6) were implanted orthotopically into the gastric wall of nude mice. Every 7 days after transplantation, five animals were

Table 1. Comparison of the survival and metastatic behavior of animals following orthotopic implantation of the highly metastatic and the parent cell lines

Cell line	Survival days	Tumor formation*	Ascites†	Disseminated metastasis				Lymph node	Liver	Pancreas‡	Kidney‡
				Omentum	Mesenterium	Peritoneum	Diaphragm				
44As3	35 ± 15 (22-65)	15/15 (100%)	14/15 (93%)	15/15	15/15	15/15	9/15	15/15	10/15	6/15	1/15
HSC-44PE	135 ± 48 (90-200)	10/15 (67%)	0/10 (0%)	5/10	3/10	3/10	0/10	5/10	0/10	0/10	0/10

*Mice were sacrificed 200 days after the orthotopic implantation. Data are the number of mice bearing metastases at the site/total number of mice bearing tumor.

†Ascites formation: >0.5 mL of ascitic fluid.

‡Micrometastases.

Table 2. Detection of metastasis and peritoneal dissemination after the orthotopic implantation of 44As3 cells

Days	Stomach	Ascites*	Disseminated metastasis				Lymph node	Liver	Pancreas†	Kidney†
			Omentum	Mesenterium	Peritoneum	Diaphragm				
7	5/5	0/5	0/5	0/5	0/5	0/5	0/5	0/5	0/5	0/5
14	5/5	0/5	3/5	0/5	0/5	0/5	1/5†	0/5	1/5	0/5
21	5/5	1/5	5/5	3/5	3/5	0/5	2/5	1/5	1/5	0/5
28	5/5	3/5	5/5	5/5	5/5	2/5	5/5	1/5	2/5	0/5
35	5/5	5/5	5/5	5/5	5/5	3/5	5/5	2/5	2/5	1/5

*Ascites formation: >0.5 mL of ascitic fluid.
†Micrometastases.

sacrificed and subjected to postmortem examination for macroscopic, histopathologic, and ultrastructural analyses (Table 2; Fig. 2). The metastatic cells (44As3) proliferated actively in the submucous tissue of the stomach (Fig. 2*A*) and began to infiltrate in the lymphatics on the 7th day. During the 2nd week following transplantation, the tumor grew more rapidly within the gastric wall, with invasion of the muscularis propria and the subserosal tissue (Fig. 2*B*). In some mice showing rapid growth of the tumor, the cancer cells broke through the serosa to become exfoliated and freed (Fig. 2*C*). These exfoliated and freed cancer cells could be visualized under the scanning electron microscope (Fig. 2*D* and *E*). Peritoneal dissemination began to be noted in the 2nd week, with cells on the greater omentum (Table 2). Micrometastases to the lymph nodes and pancreas were also noted, although not frequently. By the 3rd week, the foci of metastasis were noted in the greater omentum, mesenterium, and peritoneum. Scanning electron microscopy revealed the proliferation of the cancer cells (e.g., those colonizing the mesenterium) with the formation of larger cell clusters (data not shown). In the peritoneum, colonization of the freed cancer cells and their interaction with

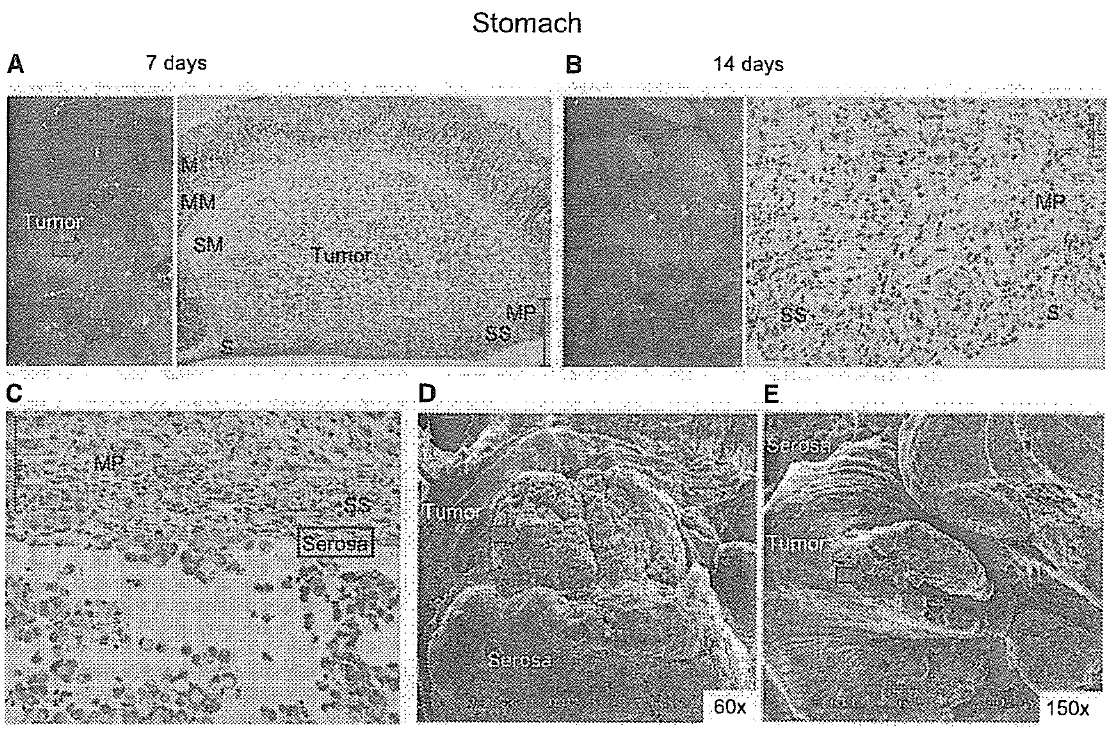

Figure 2. Macroscopic and microscopic appearance of the tumor growth of stomach of nude mice after orthotopic implantation of 44As3 cells. *A, green arrow,* orthotopic implantation of 44As3 cells in the stomach of nude mice was followed by tumor formation 7 days later. Actively proliferating 44As3 cells in the gastric submucosa (H&E). *M,* mucosa; *MM,* muscularis mucosae; *SM,* submucosa; *MP,* muscularis propria; *SS,* subserosa; *S,* serosa. *B,* tumor invasion of the muscularis propria and subserosal tissue (H&E). *C,* note 44As3 cells breaking through the serosa and becoming exfoliated and free (H&E). *D* and *E,* visualization of cancer cells breaking through the serosa and becoming exfoliated and free. Mice were sacrificed, and the tissues were examined for metastasis in various organs and processed for histologic examination as described (47, 48). Scanning electron microscopic examination was done according to standard procedures (49).

mesothelial cells were visualized (data not shown). By the 4th week, metastases to the greater omentum, mesenterium, peritoneum, and lymph nodes were noted and some animals also showed additional metastasis to the diaphragm (Table 2). Metastasis to the liver was occasionally seen. In some mice, in which the tumors grew rapidly, formation of ascites began to be noted ~21 days after the orthotopic implantation. Some of these animals became moribund on the 28th day (Tables 1 and 2). By the 35th day, all the animals showed metastasis, with dissemination to the greater omentum, mesenterium, and peritoneum accompanied by the formation of bloody ascites as well as lymph node metastasis (Table 2). Metastasis to the diaphragm was also seen frequently. Micrometastasis to the kidneys was noted in a few animals.

Analysis of the progression of dissemination using luciferase gene–tranfected cells. The analytic method described above allows detailed evaluation even of micrometastases. However, it has limitations from the viewpoint of quantitative and objective analysis. To resolve these problems, we introduced the luciferase gene into the metastatic 44As3 cell line and its parent cell line HSC-44PE by means of liposome transfer; this yielded cells with high luciferase activity, 44As3Luc and HSC44Luc, respectively. When the 44As3Luc cells (1×10^6/100 μL) were implanted s.c. into nude mice, a significant correlation was observed between tumor growth (volume) and the luciferase emission level (photon number; Fig. 3). Both cell lines were therefore used for the subsequent experiments.

The metastatic 44As3Luc or its parent cell line HSC44Luc cells were implanted orthotopically into nude mice. With the light emission noted at the site of implantation, photon counting analysis was thereafter carried out at intervals of 3 or 4 days. Figure 4*A* (*top*) presents a typical example. Chronological observation of the same animals, which were kept alive, was possible by this method. The 44As3Luc cells proliferated actively in the stomach. By the 15th day after implantation, tumor invasion of the peritoneal cavity and gradual progression of dissemination and increases in the sizes of the cell clusters were observed. Around the 25th day after implantation, a marked increase in the volume of the ascitic pool was noted by macroscopic observation, and some moribund mice were observed after the 29th day. When the moribund animals were sacrificed for autopsy, dissemination to the mesenterium and parietal peritoneum was often observed, frequently accompanied by metastasis to the lymph nodes. It was confirmed anatomically and histopathologically that the light-emitting sites corresponded to the tumor-affected sites (Fig. 4*B*). On the other hand, in the animals transplanted with the HSC44Luc, the tumor growth tended to be confined to the region of the stomach where the cells had been implanted (Fig. 4*B*), with slower tumor cell proliferation. As shown in Fig. 4*A* (*bottom*), luminescence was sometimes noted in the lymph nodes around the stomach and so on, but all of these foci of metastasis had regressed by ~60 days after implantation. Moribund animals began to be observed by the 85th day, although no ascites formation was noted in any of the animals.

By plotting the number of photons against time, a tumor growth curve reflecting the progression of peritoneal dissemination was obtained. When the relative number of photons from the highly metastatic cell line 44As3Luc and its parent cell line HSC44Luc (relative to the number of photons immediately after transplantation = 100) was plotted against time, quantitative comparison of the extents of proliferation of the two cell lines with different metastasizing potentials was possible (Fig. 4*C*).

Evaluation of the possibility of quantitative and objective screening of the effectiveness of anticancer agents. In a previous study, tumor growth was found to be suppressed in animals given i.v. injections of CPT-11, resulting in a significant prolongation

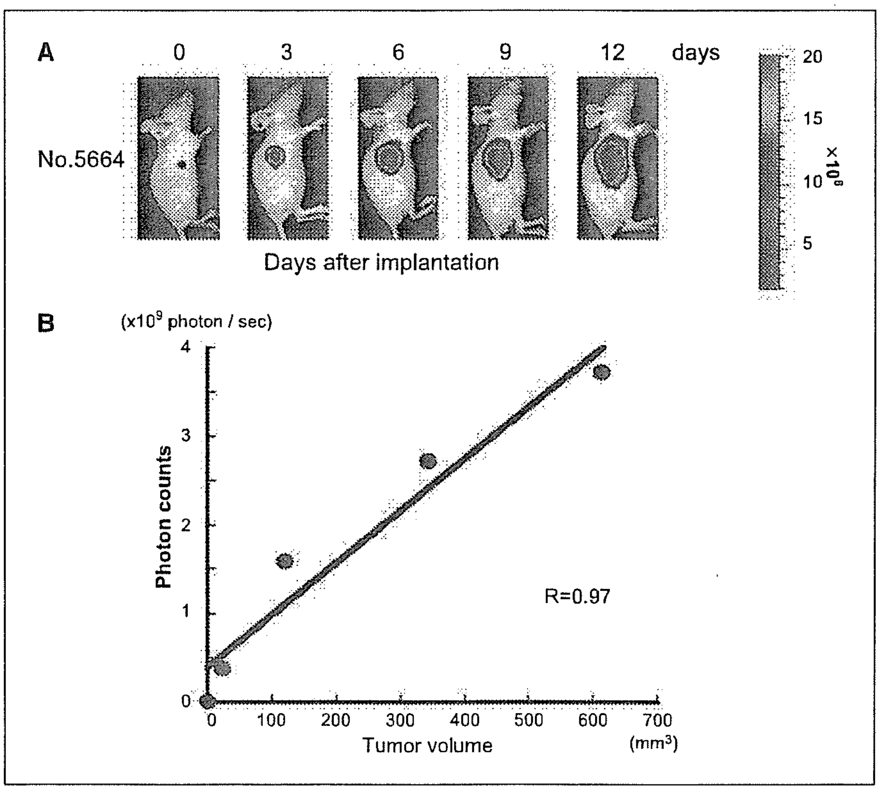

Figure 3. Correlation between the photon counts and tumor volume. *A*, nude mice bearing 44As3Luc tumors in the s.c. were visualized in anesthetized animals after i.p. inoculation of luciferin. *B*, correlation plot; strong correlation (R = 0.97) was observed between the conventional methods and our photon counting analysis method for monitoring the growth of a s.c. 44As3Luc tumor (n = 5). The tumor mass was measured at predetermined time intervals in two dimensions with calipers, and the tumor volume was calculated according to the equation ($l \times w^2$) / 2, where l is the length and w is the width (16).

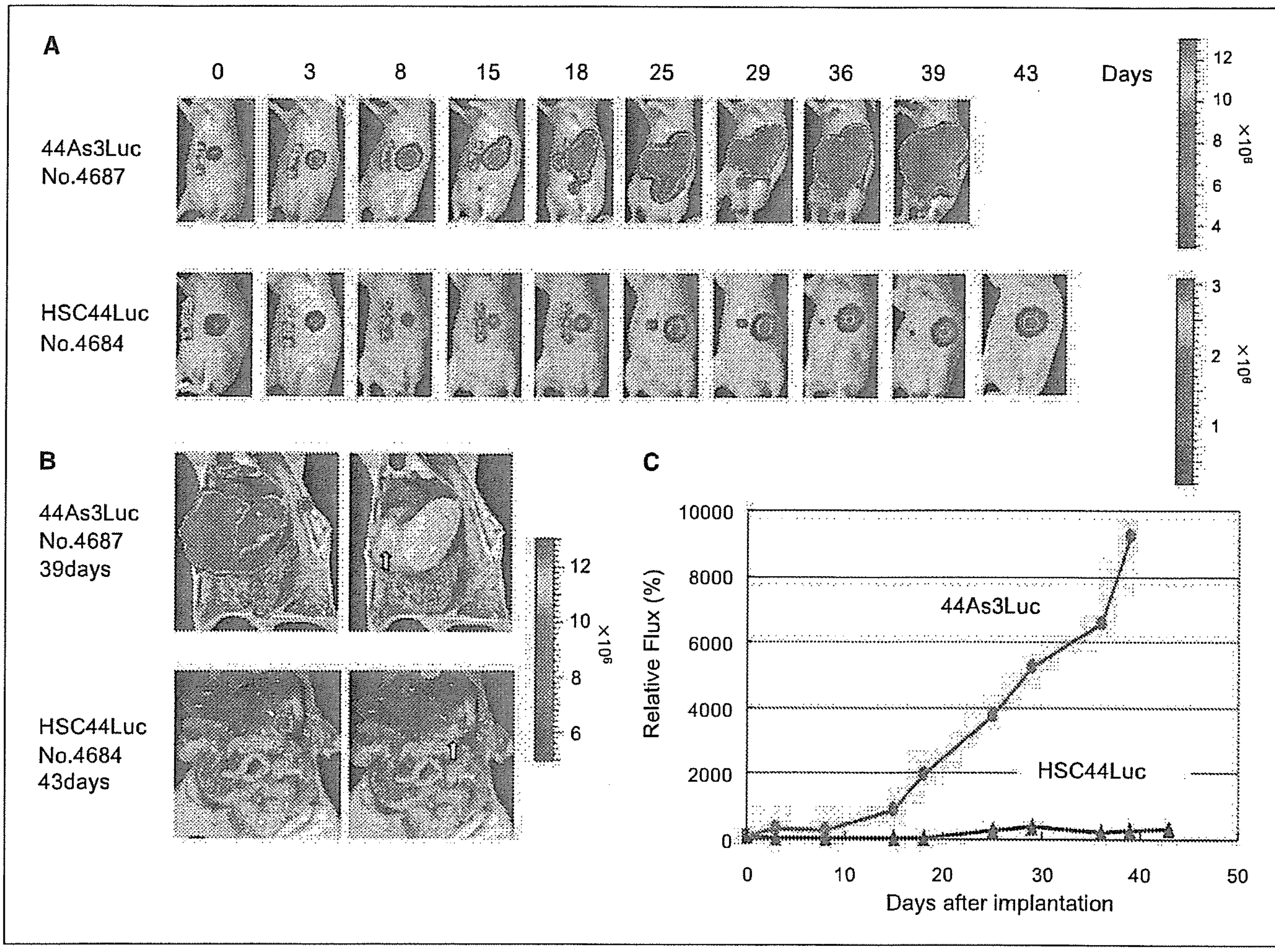

Figure 4. Quantitative photon counting analysis of progression process of peritoneal disseminated metastasis of the highly metastatic and the parent cell lines. *A,* detection of progression process of peritoneal disseminated metastasis. *B,* photon counting analysis of the peritoneal disseminations after orthotopic implantation (*yellow arrow*, site) of the cells. *C,* quantitative analysis of progression process of peritoneal disseminated metastasis of 44As3Luc (●) and HSC44Luc (▲) cell lines (n = 5). This experiment was repeated thrice, and similar results were observed each time.

of the survival period (17). A similar evaluation was conducted in the present study using 44As3Luc cells. Figure 5 (*top*) shows a typical example of the photon counting analysis, whereas Figure 5 (*bottom*) shows the time course of the changes in the number of photons. Following three doses of CPT-11 (200 mg/kg/mouse), the tumor gradually decreased in size, reaching a level close to the limit of detection on the 20th day. During the 5th and 6th week, the tumor began to show slow growth in the stomach followed during the 8th/9th week by peritoneal invasion and the onset of cancerous peritonitis accompanied by ascites formation and death of the animals. The survival period was markedly longer in the drug-treated group compared with that in the saline-treated controls. Plotting of the number of photons measured (average of five animals) against time yielded a tumor growth curve, thus allowing quantitative evaluation of drug-induced suppression of the progression of peritoneal dissemination (Fig. 5, *bottom*).

As stated above, the 44As3Luc cells began to proliferate again during the 5th/6th week after implantation in the CPT-11 treatment group. We therefore gave three additional doses beginning on day 28 (after the onset of reproliferation). Figure 5 (*top*) shows a typical example of the bioluminescence signal in such a case. The additional doses of CPT-11 (400 mg/kg/mouse) markedly suppressed the proliferation of the 44As3Luc cells until around day 60; however, proliferation again began to be detected thereafter. By around day 80, the tumor started to grow more rapidly and spread, causing moribund animals to appear by around day 90. The survival period of the animals was markedly prolonged by the additional drug doses. Figure 5 (*bottom*) shows the time course of changes in the number of photons (average of five animals). Quantitative comparison of the proliferation and spread of the tumor cells was possible between the drug treatment group and the control group and between two drug treatment groups, thus allowing objective evaluation of the responses to treatment.

Discussion

Before the present study, very little was known about how scirrhous gastric carcinoma cells invaded and proliferated within the primary lesion, how they exfoliated and thus became free, how they colonized and proliferated within the peritoneal cavity, or how they advanced to the stage of cancerous peritonitis. Herein, we investigated the course of proliferation and spread of gastric cancer

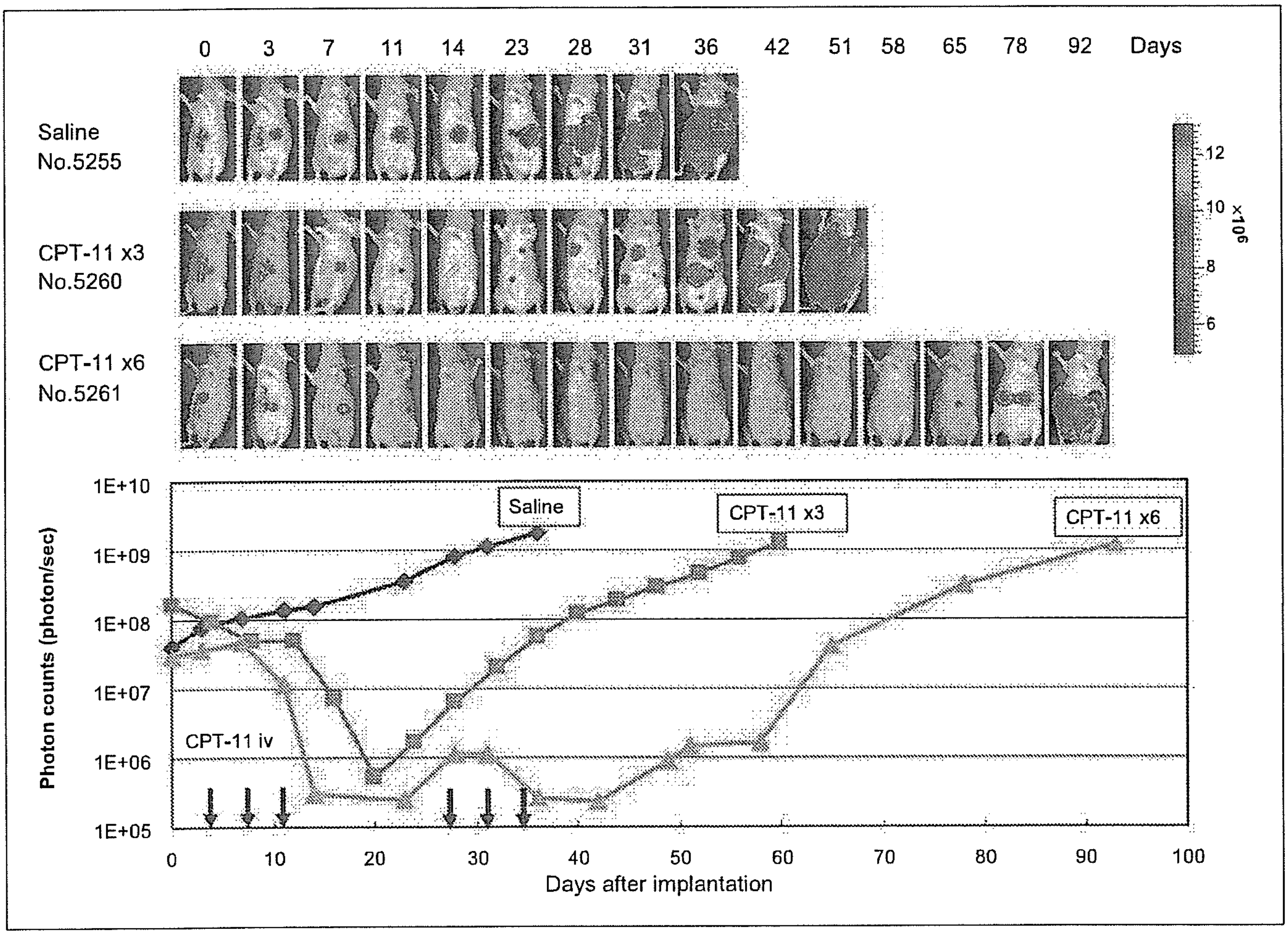

Figure 5. Quantitative photon counting analysis of the effect of CPT-11 on peritoneal disseminated metastasis 44As3Luc mouse model. Effects of CPT-11 in the peritoneal dissemination mouse model established using orthotopically implanted 44As3Luc cells. Mice receiving CPT-11 (*arrow*) or vehicle alone as control ($n = 5$; $P < 0.001$) were monitored twice weekly for the development of peritoneal dissemination. Similar results were obtained in a second experiment conducted independently.

cells by sacrificing the animals at different points of time after orthotopic implantation of the highly metastatic tumor cell line 44As3 (17) and conducted anatomic and histopathologic examinations in the sacrificed animals. In this experiment, the sequence of findings seems to endorse the previous contention that gastric cancer cells invade deeper layers of the gastric wall to reach the serosa and then exfoliate, thereby being released into the peritoneal cavity, resulting in peritoneal dissemination.

The growth of tumors in the gastric wall and the subsequent progression to cancerous peritonitis are difficult to monitor extracorporeally unlike s.c. tumors. For monitoring the progression of tumor dissemination, the only possible method was to implant the tumor cells into groups of mice and sacrifice the animals at different points of time for autopsy and observation; quantitative comparison was still not possible by this method (10–12, 18–25). All of these problems were resolved in the present study by introduction of the luciferase gene into tumor cells with a high metastasizing potential and subsequent *in vivo* photon counting analysis. In the first step, we confirmed that the results of the conventional method of evaluation in relation to proliferation of our gastric carcinoma cells were consistent with the results of our photon counting analysis. We then conducted an experiment on a model of peritoneal dissemination. Using the *in vivo* photon counting technique, it was possible to observe the same animals successively, beginning from the growth of the tumor at the site of implantation to peritoneal dissemination and, finally, the formation of ascites. Furthermore, it was possible to observe the processes of dissemination progression on a real-time basis, allowing quantitative analysis and comparison of the course of proliferation and progression within the living body after implantation of a cell line with high metastasizing potential and its parent cell line based on changes in the photon number.

Needless to say, it is important to develop a screening model for exploring substances effective against tumors and ultimately developing clinically useful anticancer agents. We previously reported that an animal model of peritoneal dissemination established using the highly metastatic cell lines (44As3, 58As1, and 58As9) established by our group satisfied all of the requirements of a model for drug screening (17, 44). However, before this model can be applied as a universally valid drug evaluation system, the following problems must be resolved: (*a*) methods for appropriate observation and objective evaluation are urgently needed, (*b*) excellent operative skill is indispensable for orthotopic implantation with high reproducibility, and (*c*) large numbers of animals are needed. With the establishment of this experimental system, the conventional problems associated with the evaluation of peritoneal dissemination have been overcome and highly reliable data are now obtainable. Therefore, a stage has been reached where this model of peritoneal dissemination can also be applied as a system for evaluation of the effects of drugs. Furthermore, because photon counting analysis allows noninvasive evaluation of the fate of cancer cells *in vivo* on a real-time basis, the pain experienced by experimental animals may be reduced, such that this technique would also be useful from the viewpoint of animal welfare (45).

We have used the bioluminescence signal from the luciferase reporter gene in our peritoneal metastasis model. Luciferase genes in our tumor cells can function stably over significant periods in tumors and in their metastases. To date, several other peritoneal metastasis models of human stomach cancer in animals have been reported (28, 31). For example, Hasegawa et al. (28) used green fluorescent protein (GFP) retroviral-infected human stomach cancer. In this nude mouse model, tumor cells were peritoneally injected and GFP transduction allowed visualization of the subsequent metastatic process. A major advantage of GFP labeling is that imaging requires no preparative procedures and hence allows for direct visualization in living tissue (26, 27, 29, 32, 34). In contrast, photon counting technique requires exogenous injection of luciferin substrate, which can stress the animals, and in addition, the intensity of the luciferase signal may sometimes be variable and unstable (46). Furthermore, Ray et al. (32) reported that red fluorescent protein imaging is ~1,000 times stronger than that of luciferase *in vivo*. Therefore, for monitoring the tumor metastasis process at the single-cell level, fluorescence imaging may be the more practical method. In fact, fluorescence-based orthotopic metastatic models have been used to study mechanisms and for drug discovery (14, 30, 33, 35).

In conclusion, our photon counting analysis involving a highly metastatic cell line, 44As3Luc, seems to be a useful model for studies, such as those designed to clarify the mechanism of peritoneal dissemination progression in intractable scirrhous gastric carcinoma, and for the development of new agents effective against such tumors.

Acknowledgments

Received 9/22/2005; revised 3/23/2006; accepted 5/26/2006.

Grant support: Ministry of Health, Labor, and Welfare of Japan Grant-in-Aid for Cancer Research.

The costs of publication of this article were defrayed in part by the payment of page charges. This article must therefore be hereby marked *advertisement* in accordance with 18 U.S.C. Section 1734 solely to indicate this fact.

We thank Dr. A. Ochiai (Pathology Division, Research Center for Innovative Oncology, National Cancer Center at Kashiwa, Kashiwa, Japan) for helpful discussions, Dr. S. Hirohashi for generous help, and M. Kodama for excellent technical work.

References

1. Chu ZD, Lang NP, Thompson C, et al. Peritoneal carcinomatosis in nongynecological malignancy. A prospective study of prognostic factors. Cancer 1989; 63:364–7.
2. Moriguchi S, Maehara Y, Korenaga D, et al. Risk factors which predict pattern of recurrence after curative surgery for patients with advanced gastric cancer. Surg Oncol 1992;1:341–6.
3. Averbach AM, Jacquet P. Strategies to decrease the incidence of intra-abdominal recurrence in resectable gastric cancer. Br J Surg 1996;83:726–33.
4. Tanahashi H, Konishi M, Nakagohri T, et al. Aggressive multimodal treatment for peritoneal dissemination and needle tract implantation of hepatocellular carcinoma: a case report. Jpn J Clin Oncol 2004;34:551–5.
5. Heintz AP. Surgery in advanced ovarian carcinoma: is there proof to show the benefit? Eur J Surg Oncol 1988; 14:91–9.
6. Hoskins WJ. Prospective on ovarian cancer: why prevent? J Cell Biochem Suppl 1995;23:189–99.
7. Kaibara N, Iitsuka Y, Kimura A, et al. Relationship between area of serosal invasion and prognosis in patients with gastric carcinoma. Cancer 1987;60:136–9.
8. Hamazoe R, Maeta M, Kaibara N. Intraperitoneal thermochemotherapy for prevention of peritoneal recurrence of gastric cancer. Final results of a randomized controlled study. Cancer 1994;73:2048–52.
9. Katano M, Morisaki T. The past, the present, and future of the OK-432 therapy for patients with malignant effusions. Anticancer Res 1998;18:3917–25.
10. Kotanagi H, Saito Y, Shinozawa N, Koyama K. Establishment of a human cancer cell line with high potential for peritoneal dissemination. J Gastroenterol 1995;30:437–8.
11. Kaneko K, Yano M, Tsujinaka T, et al. Establishment of a visible peritoneal micrometastatic model from a gastric adenocarcinoma cell line by green fluorescent protein. Int J Oncol 2000;16:893–8.
12. Nomura H, Nishimori H, Yasoshima T, et al. A novel experimental mouse model of peritoneal dissemination of human gastric cancer cells: analysis of the mechanism of peritoneal dissemination using cDNA macroarrays. Jpn J Cancer Res 2001;92:748–54.
13. Furukawa T, Fu X, Kubota T, et al. Nude mouse metastatic models of human stomach cancer constructed using orthotopic implantation of histologically intact tissue. Cancer Res 1993;53:1204–8.
14. Hoffman RM. Orthotopic metastatic mouse models for anticancer drug discovery and evaluation: a bridge to the clinic. Invest New Drugs 1999;17:343–59.
15. Yashiro M, Chung YS, Nishimura S, et al. Peritoneal metastatic model for human scirrhous gastric carcinoma in nude mice. Clin Exp Metastasis 1996;14:43–54.
16. Yanagihara K, Tanaka H, Takigahira M, et al. Establishment of two cell lines from human gastric scirrhous carcinoma that possess the potential to metastasize spontaneously in nude mice. Cancer Sci 2004;95:575–82.
17. Yanagihara K, Takigahira M, Tanaka H, et al. Development and biological analysis of peritoneal metastasis mouse models for human scirrhous stomach cancer. Cancer Sci 2005;96:323–32.
18. Fujita S, Suzuki H, Kinoshita M, Hirohashi S. Inhibition of cell attachment, invasion, and metastasis of human carcinoma cells by anti-integrin β_1 subunit antibody. Jpn J Cancer Res 1992;83:1317–26.
19. Nakashio T, Narita T, Akiyama S, et al. Adhesion molecules and TGF-β1 are involved in the peritoneal dissemination of NUGC-4 human gastric cancer cells. Int J Cancer 1997;70:612–8.
20. Ishii Y, Ochiai A, Yamada T, et al. Integrin $\alpha_6\beta_4$ as a suppressor and a predictive marker for peritoneal dissemination in human gastric cancer. Gastroenterology 2000;118:497–506.
21. Nishimura S, Adachi M, Ishida T, et al. Adenovirus-mediated transfection of caspase-8 augments anoikis and inhibits peritoneal dissemination of human gastric carcinoma cells. Cancer Res 2001;61:7009–14.
22. Minagawa A, Otani Y, Kubota T, et al. The citrus flavonoid, nobiletin, inhibits peritoneal dissemination of human gastric carcinoma in SCID mice. Jpn J Cancer Res 2001;92:1322–8.
23. Kimata M, Otani Y, Kubota T, et al. Matrix metalloproteinase inhibitor, marimastat, decreases peritoneal spread of gastric carcinoma in nude mice. Jpn J Cancer Res 2002;93:834–41.
24. Piso P, Aselmann H, von Wasielewski R, et al. Prevention of peritoneal carcinomatosis from human gastric cancer cells by adjuvant-type intraperitoneal immunotherapy in a SCID mouse model. Eur Surg Res 2003;35:470–6.
25. Yonemura Y, Endou Y, Bando E, et al. Effect of intraperitoneal administration of docetaxel on peritoneal dissemination of gastric cancer. Cancer Lett 2004; 210:189–96.
26. Chishima T, Miyagi Y, Wang X, et al. Cancer invasion and micrometastasis visualized in live tissue by green fluorescent protein expression. Cancer Res 1997;57: 2042–7.
27. Hoffman RM. The multiple uses of fluorescent proteins to visualize cancer *in vivo*. Nat Rev Cancer 2005;5:796–806.
28. Hasegawa S, Yang M, Chishima T, et al. *In vivo* tumor delivery of the green fluorescent protein gene to report future occurrence of metastasis. Cancer Gene Ther 2000; 7:1336–40.
29. Bouvet M, Wang J, Nardin SR, et al. Real-time optical imaging of primary tumor growth and multiple metastatic events in a pancreatic cancer orthotopic model. Cancer Res 2002;62:1534–40.
30. Sun F-X, Tohgo A, Bouvet M, et al. Efficacy of camptothecin analog DX-8951f (Exatecan Mesylate) on human pancreatic cancer in an orthotopic metastatic model. Cancer Res 2003;63:80–5.
31. Nakanishi H, Mochizuki Y, Kodera Y, et al. Chemosensitivity of peritoneal micrometastases as evaluated using a green fluorescence protein (GFP)-tagged human gastric cancer cell line. Cancer Sci 2003;94:112–8.
32. Ray P, De A, Min JJ, et al. Imaging tri-fusion multimodality reporter gene expression in living subjects. Cancer Res 2004;64:1323–30.
33. Hoffman RM. Orthotopic metastatic (MetaMouse) models for discovery and development of novel chemotherapy. Methods Mol Med 2005;111:297–322.

34. Nakanishi H, Ito S, Mochizuki Y, Tatematsu M. Evaluation of chemosensitivity of micrometastases with green fluorescent protein gene-tagged tumor models in mice. Methods Mol Med 2005;111:351–62.
35. Hennig R, Ventura J, Segersvard R, et al. LY293111 improves efficacy of gemcitabine therapy on pancreatic cancer in a fluorescent orthotopic model in athymic mice. Neoplasia 2005;7:417–25.
36. Contag PR, Olomu IN, Stevenson DK, Contag CH. Bioluminescent indicators in living mammals. Nat Med 1998;4:245–7.
37. Rehemtulla A, Stegman LD, Cardozo SJ, et al. Rapid and quantitative assessment of cancer treatment response using *in vivo* bioluminescence imaging. Neoplasia 2000;2:491–5.
38. Jenkins DE, Oei Y, Hornig YS, et al. Bioluminescent imaging (BLI) to improve and refine traditional murine models of tumor growth and metastasis. Clin Exp Metastasis 2003;20:733–44.
39. Vooijs M, Jonkers J, Lyons S, Berns A. Noninvasive imaging of spontaneous retinoblastoma pathway-dependent tumors in mice. Cancer Res 2002;62:1862–7.
40. Takeshita F, Minakuchi Y, Nagahara S, et al. Efficient delivery of small interfering RNA to bone-metastatic tumors by using atelocollagen *in vivo*. Proc Natl Acad Sci USA 2005;102:12177–82.
41. Lyons SK. Advances in imaging mouse tumour models *in vivo*. J Pathol 2005;205:194–205.
42. Hiraga T, Williams PJ, Ueda A, et al. Zoledronic acid inhibits visceral metastases in the 4T1/luc mouse breast cancer model. Clin Cancer Res 2004;10:4559–67.
43. Laurie NA, Gray JK, Zhang J, et al. Topotecan combination chemotherapy in two new rodent models of retinoblastoma. Clin Cancer Res 2005;11:7569–78.
44. Arao T, Yanagihara K, Takigahira M, et al. ZD6474 inhibits tumor growth and intraperitoneal dissemination in a highly metastatic orthotopic gastric cancer model. Int J Cancer 2006;118:483–9.
45. El Hilali N, Rubio N, Martinez-Villacampa M, Blanco J. Combined noninvasive imaging and luminometric quantification of luciferase-labeled human prostate tumors and metastases. Lab Invest 2002;82:1563–71.
46. Burgos JS, Rosol M, Moats RA, et al. Time course of bioluminescent signal in orthotopic and heterotopic brain tumors in nude mice. Biotechniques 2003;34:1184–8.
47. Yanagihara K, Seyama T, Tsumuraya M, et al. Establishment and characterization of human signet ring cell gastric carcinoma cell lines with amplification of the *c-myc* oncogene. Cancer Res 1991;51:381–6.
48. Yanagihara K, Kajitani T, Kamiya K, Yokoro K. *In vitro* studies on the mechanism of leukemogenesis-I. Establishment and characterization of cell lines derived from the thymic epithelial reticulum cell of the mouse. Leuk Res 1981;5:321–9.
49. Domagala W, Koss LG. Surface configuration of mesothelial cells in effusions. A comparative light microscopic and scanning electron microscopic study. Virchows Arch B Cell Pathol Incl Mol Pathol 1979;30:231–43.

Detection of Epidermal Growth Factor Receptor Mutations in Serum as a Predictor of the Response to Gefitinib in Patients with Non-Small-Cell Lung Cancer

Hideharu Kimura,[1,4,5] Kazuo Kasahara,[5] Makoto Kawaishi,[1,2] Hideo Kunitoh,[2] Tomohide Tamura,[2] Brian Holloway,[6] and Kazuto Nishio[1,3,4]

Abstract Cases of non-small-cell lung cancer (NSCLC) carrying the somatic mutation of epidermal growth factor receptor (EGFR) have been shown to be hyperresponsive to the EGFR tyrosine kinase inhibitor gefitinib (IRESSA). If EGFR mutations can be observed in serum DNA, this could serve as a noninvasive source of information on the genotype of the original tumor cells that could influence treatment and the ability to predict patient response to gefitinib. Serum genomic DNA was obtained from Japanese patients with NSCLC before first-line gefitinib monotherapy. Scorpion Amplified Refractory Mutation System technology was used to detect EGFR mutations. Wild-type EGFR was detected in all of the 27 serum samples. EGFR mutations were detected in 13 of 27 (48.1%) patients and two major EGFR mutations were identified (E746A750del and L858R). The EGFR mutations were seen significantly more frequently in patients with a partial response than in patients with stable disease or progressive disease ($P = 0.046$, Fisher's exact test). The median progression-free survival was significantly longer in patients with EGFR mutations than in patients without EGFR mutations (200 versus 46 days; $P = 0.005$, log-rank test). The median survival was 611 days in patients with EGFR mutations and 232 days in patients without EGFR mutations ($P > 0.05$). In pairs of tumor and serum samples obtained from 11 patients, the EGFR mutation status in the tumors was consistent with those in the serum of 8 of 11 (72.7%) of the paired samples. Thus, EGFR mutations were detectable using Scorpion Amplified Refractory Mutation System technology in serum DNA from patients with NSCLC. These results suggest that patients with EGFR mutations seem to have better outcomes with gefitinib treatment, in terms of progression-free survival, overall survival, and response, than those patients without EGFR mutations.

Lung cancer is a major cause of cancer-related mortality worldwide and is expected to remain a major health problem for the foreseeable future (1). Targeting the epidermal growth factor receptor (EGFR) is an appealing strategy for the treatment of non-small-cell lung cancer (NSCLC) as EGFR has been found to be expressed, sometimes strongly, in NSCLC tumors (2). Mutations of EGFR tyrosine kinase have been reported in NSCLC patients with dramatic responses to gefitinib (IRESSA), an EGFR tyrosine kinase inhibitor (3, 4). Studies have reported that EGFR mutations are strong determinants of tumor response to EGFR tyrosine kinase inhibitors (5-7). Approximately 30 mutations in exons 18 to 21 of EGFR were detected in a lung tumor specimen (3-8). The two most common NSCLC-associated EGFR mutations are the 15-bp nucleotide in-frame deletion in exon 19 (E746_A750del) and the point mutation replacing leucine with arginine at codon 858 in exon 21 (L858R; refs. 5, 8). These two mutations account for ~90% of all EGFR mutations and could explain the dramatic responders to gefitinib. Most EGFR mutations have been identified retrospectively from operative resected tumor samples. However, it is sometimes difficult to obtain tumor samples from patients with inoperable NSCLC in prospective studies; thus, it is necessary to establish a method to detect mutant EGFR, especially the two major mutations, from other more readily accessible patient samples.

Recently, PCR technology for the amplification of small amounts of DNA has made it possible to identify the same alterations, which are typically observed in DNA from resected or biopsied tumor cells, using serum samples from patients with various types of tumor, including NSCLC (9, 10). The detection of EGFR mutations in serum DNA may provide a noninvasive and repeatable source of genotypic information

Authors' Affiliations: [1]Shien-Lab, [2]Medical Oncology, National Cancer Center Hospital; [3]Pharmacology Division and [4]Center for Medical Genomics, National Cancer Center Research Institute, Tokyo, Japan; [5]Respiratory Medicine, Kanazawa University Hospital, Ishikawa, Japan; and [6]AstraZeneca, Alderley Park, Cheshire, United Kingdom

Received 10/27/05; revised 1/30/06; accepted 2/15/06.

Grant support: Research Resident Fellowship from the Foundation for Promotion of Cancer Research (Japan) for the 3rd Term Comprehensive 10-Year Strategy for Cancer Control (H. Kimura).

The costs of publication of this article were defrayed in part by the payment of page charges. This article must therefore be hereby marked *advertisement* in accordance with 18 U.S.C. Section 1734 solely to indicate this fact.

Note: IRESSA is a trademark of the AstraZeneca group of companies.

Requests for reprints: Kazuto Nishio, Shien-Lab, Medical Oncology, National Cancer Center Hospital, Tsukiji 5-1-1, Chuo-ku, Tokyo, Japan. Phone: 81-3-3542-2511; Fax: 81-3-3542-1886; E-mail: knishio@gan2.res.ncc.go.jp.

doi:10.1158/1078-0432.CCR-05-2324

that could influence treatment and prognosis, especially in patients with NSCLC treated with gefitinib. However, it is well known that interfusion of normal cells with tumor cells prevents the detection of mutations in the tumor cells. Therefore, it is necessary to enhance the sensitivity of the detection of EGFR mutations from tumor-derived DNA mixed with normal cells.

Scorpion primers are used in a fluorescence-based method for the specific detection of PCR products (11). A Scorpion is a specific probe sequence that is held in a hairpin loop configuration by complementary stem sequences at the 5' and 3' ends of the probe. Scorpion can be used in combination with the Amplified Refractory Mutation System (ARMS) to enable the detection of single-base mutations (11, 12). ARMS technology is used for allele discrimination and additional mismatches are introduced near the 3' terminus of the primers to enhance specificity. For the detection of known mutations, the Scorpion-ARMS method is highly sensitive and fast (13). Our hypothesis was that the ARMS and Scorpion methods could enhance the sensitivity of the detection of EGFR mutations from the wild type.

The aims of this study were to develop a highly sensitive assay for the detection of EGFR mutations in serum DNA, to compare the mutation status in serum to tumors from a subset of their patients, and to clarify the relationship between the EGFR mutation status in serum DNA and clinical manifestations, and in particular the responsiveness to gefitinib.

Materials and Methods

Patients and clinical trials. This study was carried out as a correlative study in a multicenter clinical phase II trial of gefitinib monotherapy at the Department of Respiratory Medicine, Kanzawa University Hospital; the Department of Internal Medicine, Kouseiren Takaoka Hospital; the Department of Internal Medicine, Shinminato Municipal Hospital; the Department of Internal Medicine, Fukuiken Saiseikai Hospital; the Department of Respiratory Medicine, Toyama City Hospital; the Department of Respiratory Medicine, Ishikawa Prefectoral Hospital; and the Department of Respiratory Medicine, Kanazawa Municipal Hospital. According to Simon's minimax design, our study, with a sample size of 25, had an 80% power to support the hypothesis that the true objective response rate was >30% and a 5% significance to deny the hypothesis that the true objective response rate was <10%. Assuming an inevaluability rate of <20%, we projected an accrual of 30 patients. The study was conducted with the approval of the appropriate ethical review boards based on the recommendations of the Declaration of Helsinki for biomedical research involving human subjects. Japanese patients with stage IIIB or IV histologically or cytologically proven chemotherapy-naïve NSCLC were enrolled in this trial. Gefitinib was orally given to all patients at a fixed dosage of 250 mg/d. Efficacy was assessed using the Response Evaluation Criteria in Solid Tumors guidelines (14). The analysis of the samples in this study was done blinded to the clinical outcome.

Blood sample collection and DNA extraction. Blood samples from the 27 patients with NSCLC were collected before the initiation of gefitinib administration. Separated serum was stocked at −80°C until use. Serum DNA was extracted and purified using a Qiamp Blood Kit (Qiagen, Hilden, Germany) with the following protocol modifications. One column was used repeatedly until the whole sample had been processed. The resulting DNA was eluted in 50 μL of sterile bidistilled buffer. The concentration and purity of the extracted DNA were determined by spectrophotometry. The extracted DNA was stocked at −20°C until use.

Scorpion ARMS primers for the detection of E746_A750del and L858R. We used an EGFR Scorpion Kit (DxS Ltd., Manchester, United Kingdom), which combined two technologies (i.e., ARMS and Scorpion) to detect mutations in real-time PCR reactions. Four kinds of scorpion primers for the detection of E746_A750del, L858R, and wild type in both exon 19 and exon 21 were designed and synthesized by DxS. The sequences of the scorpion primer for E746_A750del and L858R were based on the GenBank-archived human sequence for EGFR (accession no. AY588246). All reactions were done in 25-μL volumes using 1 μL of template DNA, 7.5 μL of reaction buffer mix, 0.6 μL of primer mix, and 0.1 μL of Taq polymerase. All reagents are included in this kit. Real-time PCR was carried out using SmartCycler II (Cepheid, Sunnyvale, CA) under the following conditions: initial denaturation at 95°C for 10 minutes, 50 cycles of 95°C for 30 seconds, and 62°C for 60 seconds with fluorescence reading (set to FAM that allows optical excitation at 480 nm and measurement at 520 nm) at the end of each cycle. Data analysis was done with Cepheid SmartCycler software (Ver. 1.2b). The cycle threshold (Ct) was defined as the cycle at the highest peak of the second derivative curve, which represented the point of maximum curvature of the growth curve. Both Ct and maximum fluorescence (Fl) were used for interpretation of the results. Positive results were defined as follows: Ct ≤45 and Fl ≥50. These analyses were done in duplicate for each sample and reviewed by two investigators blinded to any clinical information. To confirm the sensitivities for the detection of E746_A750del and L858R, we used the standard DNA that was included in the EGFR Scorpion Kit. Standard DNA with E746_A750del and L858R at a volume of 1, 10, 100, 1,000, or 10,000 pg and the mixture of standard DNA with wild type at 10,000 pg and standard DNA with E746_A750del and L858R at a volume of 1, 10, 100, 1,000 or 10,000 pg were used. For quantification, a standard curve was generated by plotting the cycle number of Ct against the log of the DNA volume of the known standards. The linear correlation coefficient (R^2) values and the formula of the slopes were calculated. DNA (10,000 pg) for the positive control was extracted from a Japanese human adenocarcinoma PC-9 cell line known to contain E746_A750del, a Japanese human adenocarcinoma 11_18 cell line known to contain L858R, and a human epidermoid carcinoma A431 cell line known to contain wild-type exon 19.

Tissue sample collection and DNA extraction. Tumor specimens were obtained on protocols approved by the Institutional Review Board. Twenty paraffin blocks of tumor material, obtained from 15 patients at the time of diagnoses (and before treatment), were collected retrospectively. Eleven tumor samples were collected from the primary cancer via transbronchial lung biopsy, one was resected intraoperatively, and nine were from metastatic sites (four from bone, three lymph nodes, one brain, and one colon). All specimens underwent histologic examination to confirm the diagnosis of NSCLC. DNA extraction from tumor samples was done using a DEXPAT kit (TaKaRa Biomedicals, Shiga, Japan).

PCR amplification and direct sequencing. Amplification and direct sequencing were done in duplicate for each sample obtained from serum and tissue specimens. PCR was done in 25-μL volumes using 15 μL of template DNA, 0.75 units of Ampli Taq Gold DNA polymerase (Perkin-Elmer, Roche Molecular Systems, Inc., Branchburg, NJ), 2.5 μL of PCR buffer, 0.8 mmol/L deoxynucleotide triphosphate, 0.5 μmol/L of each primer, and different concentrations of $MgCl_2$, depending on the polymorphic marker. The sequences of primer sets and schedules of amplifications were followed as previously described (12). The amplification was done using a thermal cycler (Perkin-Elmer, Foster City, CA). Sequencing was done using an ABI prism 310 (Applied Biosystems, Foster City, CA). The sequences were compared with the GenBank-archived human sequence for EGFR (accession no. AY588246).

Statistical analysis. Fisher's exact test was used to assess the relationship between the presence of EGFR mutations in patients with NSCLC and different characteristics, including gender, tumor histology, and response to gefitinib. Regarding analyses of response to gefitinib, patients were categorized into the two groups: (*a*) partial response and (*b*) stable disease or progressive disease (Response Evaluation Criteria in Solid Tumors criteria). We compared Kaplan-Meier curves for overall survival and progression-free survival using the standard log-rank test. Overall survival was defined as the time from the initiation of gefitinib administration to death from any cause; patients known to be still alive at the time of the analysis were censored at the time of their last follow-up. Progression-free survival was defined as the time from the initiation of gefitinib administration to first appearance of progressive disease or death from any cause; patients known to be alive and without progressive disease at the time of analysis were censored at the time of their last follow-up. $P = 0.05$ was considered statistically significant. The statistical analyses were done using the StatView software package version 5.0.

Results

Patients and extracted DNA from serum. Twenty-eight patients were enrolled between October 23, 2002 and August 3, 2003 (Table 1). All patients were evaluated for response and followed for progression-free survival and overall survival. Blood samples (2 mL) were collected from 27 of these patients before the initiation of gefitinib administration. These 27 patients represented a subset of that phase II study. Serum DNA was extracted in all 27 samples at a median concentration of 70.0 ng/mL (range, 0-1,720.0 ng/mL).

Sensitivity of the EGFR Scorpion. Preliminary experiments were done to evaluate the sensitivity of the EGFR Scorpion kit (Fig. 1A-C). All curves using E746_A750del and L858R standard DNA (volumes of 1-10,000 pg) increased up to 45 cycles (Fig. 1A). When wild-type standard DNA and distilled water were used as negative controls, the curves did not increase and continued flat at 50 cycles (Fig. 1A and C). When diluted E746_A750del and L858R standard DNA were mixed with wild-type standard DNA at ratios from 10^0 to 10^{-5}, all curves that indicated the presence of E746_A750del and L858R increased up to 45 cycles (Fig. 1B and D). Standard curves in the range of measured volumes in this study were linear with r^2 values from 0.987 to 0.998. Both slopes of curves were almost parallel (Fig. 1E). The Ct of diluted mutant standard DNA mixed with wild-type DNA was close to that of mutant standard DNA alone. Although the peak fluorescence levels of diluted E746_A750del standard DNA mixed with wild-type DNA were lower than without wild-DNA standard, the presence of E746_A750del was clearly detected at ratios less than 10^{-4}. The peak fluorescence levels of diluted L858R standard DNA mixed with wild-type DNA were equivalent to those without wild-DNA standard. Curves of DNA with the mutations at an amount of up to 1 pg were unaffected by interfusion of DNA of wild-type EGFR. There were no significant differences between either the minimum detectable volume of the mutations or the minimum detectable ratio of wild type to the mutations.

In the cell-based experiments using genomic DNA of human cancer cell lines, the signal using DNA derived from the PC-9 cells was detected whereas the signal using DNA from the A431 cells was, as expected, not detected (Fig. 1D and E).

EGFR mutation status of serum DNA detected by EGFR scorpion. The E746_A750del or L858R status of serum DNA derived from 27 patients with NSCLC was examined. Wild-type exons 19 and 21 were detected from all serum samples. E746_A750del was detected in samples of 12 patients. L858R was detected in 1 patient (Table 2). In total, EGFR mutations were detected in 13 of 27 (48.1%) patients. The histologic subtypes of the original tumors are summarized in Table 3A in the 27 patients who were assessed for EGFR mutation in serum. Eleven of 23 (47.8%) cases of adenocarcinoma, one of two cases of squamous-cell carcinoma, and one of two cases of large-cell carcinoma were positive for EGFR mutations. An EGFR mutation was more frequently detected in the samples from female patients than those from males [7 of 10 (70%) versus 6 of 17 (35%); Table 3B].

EGFR mutation status in serum (EGFR Scorpion) and response to gefitinib. EGFR mutations were more frequently observed in the samples from the patients who showed a partial response (7 of 9 cases, 77.8%) than in samples from patients with stable disease or progressive disease (6 of 18 cases, 33.3%; $P = 0.046$, Fisher's exact test; Table 3C).

EGFR mutation status in serum (EGFR Scorpion) and effect on survival. Median progression-free survival and overall survival of all the patients treated with gefitinib were 98 and 306 days, respectively. Patients with EGFR mutations in serum showed a significantly longer median progression-free survival compared with the patients without EGFR mutations (200 versus 46 days, $P = 0.005$; Fig. 2A). The patients with EGFR mutations showed a longer median overall survival compared with the patients without EGFR mutations, although there was no statistical significance (611 versus 232 days, $P = 0.078$; Fig. 2B). These results suggest that patients who were serum EGFR mutation positive seem to have better outcomes with gefitinib treatment, in terms of progression-free survival, overall survival, and response, than those patients who were EGFR mutation negative.

EGFR mutation in serum analyzed by direct sequencing and in comparison with EGFR Scorpion. The deletional mutation (E746_A750del) was detected by direct sequencing in serum DNA extracted from 10 of 27 patients (37.0%). No point mutation in exons 18, 19, and 21 was detected in the PCR

Table 1. Patient characteristics

	(*n*)
No. patients	27
Age (y)	
Median	64
Range	44-87
Sex	
Male	17
Female	10
Performance status	
0	19
1	6
2	2
Stage	
IIIB	3
IV	24
Histology	
Adenocarcinoma	23
Squamous-cell carcinoma	2
Large-cell carcinoma	2
Response	
Partial response	9
Stable disease	8
Progressive disease	10

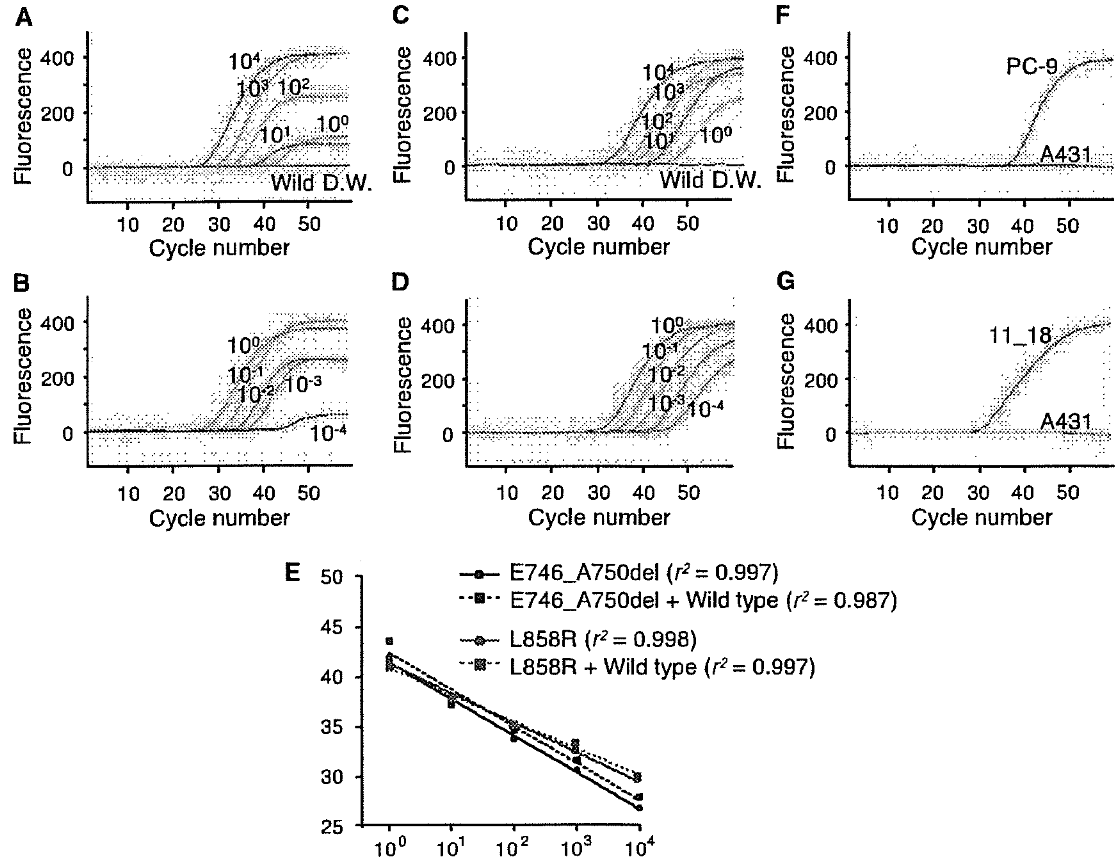

Fig. 1. Sensitivity of detection for mutations of E746_A750del and L858R using the EGFR Scorpion kit (*A* and *B*, E746_A750del; *C* and *D*, L858R). Standard DNA with E746_A750del (*A*) and L858R (*C*) were used at various volumes of 10,000 pg (10^4), 1,000 pg (10^3), 100 pg (10^2), 10 pg (10^1), and 1 pg (10^0). Standard DNA with wild-type (*Wild*) and distilled water (*D.W.*) were used as negative controls in the same experiment. Standard DNA with E746_A750del (*B*) and L858R (*D*) at concentrations from 1 to 10,000 pg were mixed with 10,000 pg of standard DNA with wild-type at a ratio of 1:1 (10^0), 1:10 (10^{-1}), 1:100 (10^{-2}), 1:1,000 (10^{-3}), and 1:10,000 (10^{-4}). *E*, standard curves were derived by plotting the Ct of each curve (shown in *A-D*) against the log of the standard DNA volume (*black lines*, E746_A750del; *blue lines*, L858R). *F*, PC-9 with E746_A750del and A431 with wild-type. *G*, 11_18 with L858R and A431.

products from serum samples. The serum EGFR status detected by direct sequence was not correlated statistically with histologic type, gender, response to gefitinib (Table 3), or survival (progression-free survival, P = 0.277; overall survival, P = 0.859). EGFR mutation status, as assessed by direct sequence, was consistent with those assessed by EGFR Scorpion in 15 of 27 (55.6%) of the paired samples. In four cases, EGFR mutation status (E746_A750del) was positive by direct sequence and negative by EGFR Scorpion. Eight cases were negative by direct sequence and positive by EGFR Scorpion. Thus, the sensitivity of EGFR Scorpion seems to be higher than that of direct sequencing due to the use of the specific primers for EGFR mutations in this kit.

EGFR mutations in tumors in comparison with those in serum. Twenty tumor samples were obtained from 15 patients retrospectively. Sequencing of EGFR exons 19 and 21 was done in samples from 12 of these under the same PCR conditions (Table 4; the other three samples were not evaluated because of low amplification of PCR products). EGFR mutations were detected in four cases (25.0%); three were the 15-bp deletion (E746_A750del) in exon 19 and one was the L858R point mutation in exon 21. Tumor histology of patients with EGFR mutations was adenocarcinoma in three and large-cell carcinoma in one. The responses to gefitinib in these four patients were two partial response, one stable disease, and one progressive disease.

Pairs of tumor samples and serum samples were obtained retrospectively from 11 patients (Table 4). The EGFR mutation status in the tumors was consistent with those in the serum of 8 of 11 (72.7%) of the paired samples. The E746_A750del mutation was positive in the tumor and negative in the serum in two patients, and the E746_A750del mutation was negative in the tumor and positive in the serum in one patient.

Discussion

Our findings have shown that EGFR mutations were detectable in serum samples obtained from patients with NSCLC and that the EGFR Scorpion kit consisting of ARMS and Scorpion technology is a useful method for detection of EGFR mutations. The EGFR mutation status in serum detected by the EGFR Scorpion was correlated statistically with responsiveness to, and the progression-free survival of, gefitinib treatment. Our finding supports the hypothesis that the EGFR mutation status from serum DNA is useful to predict the responsiveness to gefitinib.

The mutation rate observed in our study seems to be relatively high (48%) although we have detected only two major mutations. EGFR mutations have been detected at a higher frequency in lung tumors from female patients, those with adenocarcinoma histology, nonsmokers, and patients of Asian origin (6, 8). However, previous reports show that the mutation rate of EGFR in operative samples of Japanese patients was from 26% to 59% (4, 6, 15, 16). The EGFR mutation rate in our study is equivalent to that observed in these reports. It can be speculated that the high sensitivity and specificity of the EGFR Scorpion allowed us to detect the EGFR mutations even in serum. Another possible reason is the high number of patients with adenocarcinoma in our study (23 of 27, 85.2%). Previous studies have shown that very few patients with nonadenocarcinoma, including squamous cell carcinomas and large-cell carcinomas, have EGFR mutations (3-8). Our results were in line with the previous studies and showed that no patients with squamous cell carcinoma or large-cell carcinoma had the mutations.

Table 2. Patients' characteristics and EGFR mutant status detected from serum DNA using the EGFR ARMS-Scorpion method

Response	Gender	Histology	Exon 19		Exon 21	
			Wild	E746_A750del	Wild	L858R
PR	M	Ad	+	–	+	+
PR	F	Ad	+	+	+	–
PR	M	Ad	+	–	+	–
PR	F	Ad	+	+	+	–
PR	M	Ad	+	+	+	–
PR	F	Ad	+	–	+	–
PR	M	Ad	+	+	+	–
PR	F	Ad	+	+	+	–
PR	F	Ad	+	+	+	–
SD	M	Large	+	–	+	–
SD	F	Ad	+	+	+	–
SD	M	Ad	+	–	+	–
SD	F	Ad	+	–	+	–
SD	F	Ad	+	+	+	–
SD	M	Ad	+	–	+	–
SD	F	Ad	+	+	+	–
SD	M	Scc	+	+	+	–
PD	F	Scc	+	–	+	–
PD	M	Ad	+	–	+	–
PD	M	Ad	+	–	+	–
PD	M	Large	+	+	+	–
PD	M	Ad	+	–	+	–
PD	M	Ad	+	–	+	–
PD	M	Ad	+	–	+	–
PD	M	Ad	+	–	+	–
PD	M	Ad	+	+	+	–
PD	M	Ad	+	–	+	–

Abbreviations: SD, stable disease; PD, progressive disease; PR, partial response; M, male; F, female; Ad, adenocarcinoma; Large, large-cell carcinoma; Scc, squamous-cell carcinoma; +, curve detected by SmartCycler; –, curve not detected by SmartCycler.

Table 3. Frequency of EGFR mutations in serum DNA from patients with NSCLC according to histology (A), gender (B), and response to gefitinib (C)

	EGFR Scorpion kit			Direct sequence		
	+	–		+	–	
(A) Histology and EGFR mutant states						
Ad	11	12		8	15	
Non-Ad	2	2	$P > 0.999$	2	2	$P > 0.999$
(B) Gender and EGFR mutant states						
Female	7	3		5	5	
Male	6	11	$P = 0.120$	5	12	$P = 0.415$
(C) Response to gefitinib and EGFR mutant states						
PR	7	2		4	5	
SD/PD	6	12	$P = 0.046$	6	12	$P = 0.683$

NOTE: A total of 27 samples were obtained from 28 patients before treatment.

We identified 12 deletion mutations and a single point mutation (L858R). Previous reports have shown that the frequency of detection of E746_A750del is almost equivalent to that of L858R (15, 16). It seems that the rate of detection of L858R in our study was very low compared with the rate of E746_A750del. The sensitivity for detection of L858R using the Scorpion ARMS method is very high and equivalent to that of E746_A750del. We thus consider that it is unlikely that the low-frequency L858R mutation could be due to assay-related false-negative findings. On the other hand, it also seems unlikely that either sampling method or the patients' eligibility criteria are biased toward the high rate of E746_A750del. Therefore, we have not been able to clarify the moot point. Further analyses in much larger groups of patients will be necessary to clarify the frequency of the major two mutations in serum DNA. Unfortunately, parallel tumor tissue investigations were done only on a small subset of the participating patients. Furthermore, findings in the serum were divergent from those obtained from the primary tissue in 3 of 11 patients from whom the paired samples were obtained. Therefore, this study is at best hypothesis-forming and will require follow-up analysis in much larger groups of patients.

Some investigators reported that mutations in the EGFR tyrosine kinase domain enhanced responsiveness to the EGFR tyrosine kinase inhibitors gefitinib and erlotinib, and seemed to be associated with the prolonged survival of the patients who received these drugs (7, 8). In a placebo controlled study showing a survival advantage for NSCLC patients who received erlotinib, Tsao et al. (17) showed that the presence of an EGFR mutation might increase responsiveness to erlotinib, but was not indicative of a survival benefit, and concluded that EGFR mutation analysis was not necessary to identify patients in whom treatment with EGFR inhibitors was appropriate. Our results are not in line with their conclusions. In their study, the rate of mutation analysis was low and 107 of 731 patients

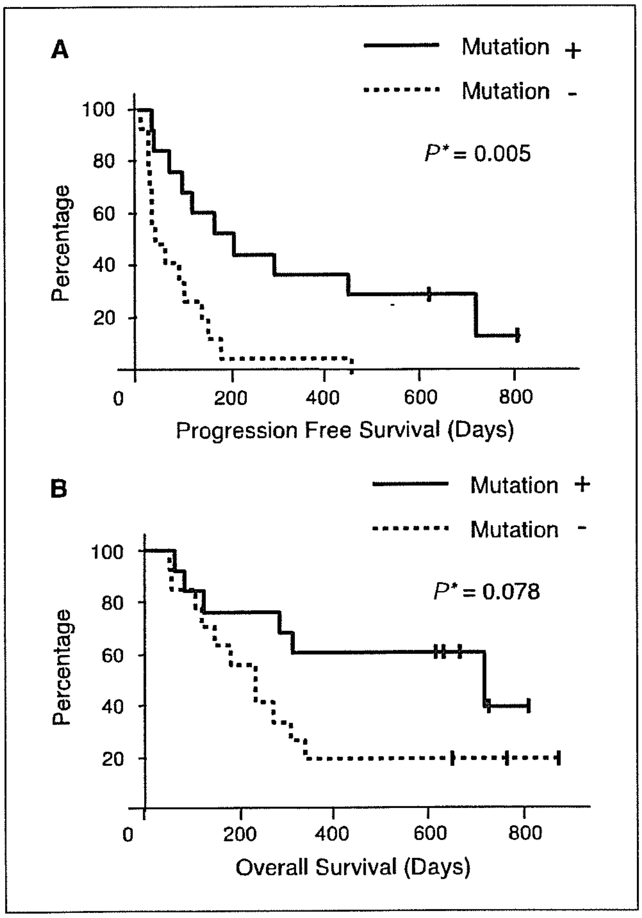

Fig. 2. Progression-free survival (*A*) and overall survival (*B*) with respect to the EGFR mutation status of NSCLC. *, log-rank test.

enrolled in their study were successfully analyzed for EGFR mutation. Sensitivity for detecting EGFR mutation in their study might be unstable as interfusion of normal cells in tumor cells decreases the sensitivity for detecting tumor-derived mutations using direct sequencing. They propose that additional processes (such as microdissection) to enrich tumor cell DNA might increase the rate of detection of new mutations; however, it seems that their results are insufficiently robust to reach this conclusion. Therefore, we propose the use of EGFR mutation analysis from serum DNA, which is easily collected and repeatable, to show that EGFR mutation status using the EGFR Scorpion kit correlates with the responsiveness to gefitinib.

EGFR mutation in NSCLC is reported to be somatic (3, 4). It is well known that the concentration of free circulating DNA in serum is higher in patients with tumors than in healthy volunteers (18) and it seems that the detected mutational EGFR in serum was tumor derived. This is the first report analyzing EGFR mutations from serum DNA and evaluating EGFR mutation status and clinical outcome (response and survival) with gefitinib. No other studies have analyzed EGFR mutations from samples other than actual tumor samples. The mutation in two patients was positive in the tumor and negative in the serum, and the mutation in one patient was negative in the tumor and positive in the serum. We have tried to explain the discrepancy why tumor and serum were not better correlated as follows. In cases of positive in the tumor and negative in the serum, the volumes of mutant DNA extracted from the serum were under the detectable limit using the Scorpion ARMS method, or a very small amount of DNA derived from an actual tumor was circulating in the blood-stream. A previous study showed that 73% of patients with at least one molecular event, such as a hypermethylation of the tumor suppressor gene *p16*, in their tumor DNA had the same alteration in plasma DNA (10). In a case of negative in the tumor and positive in the serum, wild-type DNA interfered with

Table 4. EGFR mutation status in tumor samples and serum samples. Pairs of both tumor samples and serum samples were obtained from 11 patients

Gender	Histology	Response	EGFR mutation status				
			Tumor sample	EGFR Scorpion kit (serum sample)			
				Exon 19		Exon 21	
				Wild	Mutation	Wild	Mutation
M	Large	SD	Wild	+	–	+	–
F	Scc	PD	Wild	+	–	+	–
M	Ad	PD	Wild	+	–	+	–
M	Ad	PR	L858R	+	–	+	+
F	Ad	SD	Wild*	+	+	+	–
M	Large	PD	E746-A750del	+	+	+	–
M	Ad	PD	Wild	+	–	+	–
M	Ad	PD	Wild	+	–	+	–
M	Ad	SD	E746-A750del*	+	–	+	–
F	Ad	PR	E746-A750del*	+	–	+	–
M	Ad	PD	Wild	+	–	+	–

*Patients who have different states of EGFR mutation from tumor-derived DNA and serum-derived DNA.

the detection of mutant DNA in the tumor samples using the direct sequencing method. The rate of the mutations in serum DNA detected by the Scorpion ARMS was compared with that in tumor tissues detected by the direct sequencing method as a current standard method. DNA from tumor samples consisted of a mixture of the mutant DNA and wild-type DNA because the EGFR mutation status was always heterogeneous, and the complete removal of normal cells, such as normal epithelial cells and inflammatory cells, from tumor specimens is very difficult. Parallel tumor tissue investigations were done on only a small subset of these patients, which is a recognized limitation in the present study. A larger study is necessary to evaluate the consistency of the mutation status from tumor and serum. On the other hand, it is sometimes difficult to obtain tumor samples from patients with inoperable NSCLC in prospective studies. We showed that patients who were EGFR mutation positive in the serum DNA using the Scorpion ARMS method seem to have better outcomes with gefitinib treatment in terms of progression-free survival, overall survival, and response, despite the nonconformity between the mutation states of tumor and serum DNA in some of the patients. We anticipate that the detection of EGFR mutations in serum DNA using the Scorpion ARMS will be equivalently useful as a feasible approach for predicting tumor response to gefitinib.

Two groups have reported alternative methods for detection of EGFR mutations. One group used the LightCycler PCR assay (19) and the other postulated that the SSCP assay was more sensitive than direct sequencing and was a rapid method (20). Further studies are needed to validate these assays for detection of EGFR mutations and to clarify the most sensitive assay. Although the direct sequence method is common in reported studies, the EGFR mutation status in serum DNA by direct sequencing did not correlate with the responsiveness to and survival benefit of gefitinib in our study. These results indicate that the EGFR Scorpion kit is superior to the direct sequencing method for detection of an EGFR mutation in serum as a predictive marker.

One limitation of the EGFR Scorpion kit is that it is only able to detect mutations targeted by the designed Scorpion primers. EGFR mutations are not solely at these two sites but clustered around the ATP-binding site in exons 18, 19, and 21 (3-8). Moreover, the secondary mutation, a substitution of methionine for threonine at position 790 (T790M), leads to gefitinib resistance in NSCLC patients who have EGFR mutations and are responsive to treatment with gefitinib (21-23). Mutations in *K-ras*, a known downstream signaling molecule in the EGFR signaling pathway, are more frequent in patients who develop disease progression with treatment with either gefitinib or erlotinib (24). These mutation states may also be critical factors for the treatment of gefitinib. To clarify the usefulness of serum DNA as a source of genotypic information, the Scorpion primers need to be designed for detection of these mutations, and further studies using these primers are required.

In conclusion, the two major mutations of EGFR, E746_A750del and L858R, were detected in serum DNA with the EGFR Scorpion kit from patients with NSCLC. These results suggest that patients who were EGFR mutation positive seem to have better outcomes with gefitinib treatment, in terms of progression-free survival, overall survival, and response, than those patients who were EGFR mutation negative. In the near future, a controlled clinical trial is necessary to confirm these conclusions.

References

1. Parkin DM, Bray F, Ferlay J, Pisani P. Global cancer statistics, 2002. CA Cancer J Clin 2005;55:74-108.
2. Franklin WA, Veve R, Hirsch FR, Helfrich BA, Bunn PA, Jr. Epidermal growth factor receptor family in lung cancer and premalignancy. Semin Oncol 2002; 29:3-14.
3. Lynch TJ, Bell DW, Sordella R, et al. Activating mutations in the epidermal growth factor receptor underlying responsiveness of non-small-cell lung cancer to gefitinib. N Engl J Med 2004;350:2129-39.
4. Paez JG, Janne PA, Lee JC, et al. EGFR mutations in lung cancer: correlation with clinical response to gefitinib therapy. Science 2004;304:1497-500.
5. Pao W, Miller V, Zakowski M, et al. EGF receptor gene mutations are common in lung cancers from "never smokers" and are associated with sensitivity of tumors to gefitinib and erlotinib. Proc Natl Acad Sci U S A 2004;101:13306-11.
6. Shigematsu H, Lin L, Takahashi T, et al. Clinical and biological features associated with epidermal growth factor receptor gene mutations in lung cancers. J Natl Cancer Inst 2005;97:339-46.
7. Han SW, Kim TY, Hwang PG, et al. Predictive and prognostic impact of epidermal growth factor receptor mutation in non-small-cell lung cancer patients treated with gefitinib. J Clin Oncol 2005;23:2493-501.
8. Kosaka T, Yatabe Y, Endoh H, Kuwano H, Takahashi T, Mitsudomi T. Mutations of the epidermal growth factor receptor gene in lung cancer: biological and clinical implications. Cancer Res 2004;64:8919-23.
9. Sanchez-Cespedes M, Monzo M, Rosell R, et al. Detection of chromosome 3p alterations in serum DNA of non-small-cell lung cancer patients. Ann Oncol 1998;9:113-6.
10. Esteller M, Sanchez-Cespedes M, Rosell R, Sidransky D, Baylin SB, Herman JG. Detection of aberrant promoter hypermethylation of tumor suppressor genes in serum DNA from non-small cell lung cancer patients. Cancer Res 1999;59:67-70.
11. Whitcombe D, Theaker J, Guy SP, Brown T, Little S. Detection of PCR products using self-probing amplicons and fluorescence. Nat Biotechnol 1999;17: 804-7.
12. Newton CR, Graham A, Heptinstall LE, et al. Analysis of any point mutation in DNA. The amplification refractory mutation system (ARMS). Nucleic Acids Res 1989;17:2503-16.
13. Bates JA, Taylor EA. Scorpion ARMS primers for SNP real-time PCR detection and quantification of *Pyrenophora teres*. Mol Plant Pathol 2001;2:275-80.
14. Therasse P, Arbuck SG, Eisenhauer EA, et al. New guidelines to evaluate the response to treatment in solid tumors. European Organization for Research and Treatment of Cancer, National Cancer Institute of the United States, National Cancer Institute of Canada. J Natl Cancer Inst 2000;92:205-16.
15. Mitsudomi T, Kosaka T, Endoh H, et al. Mutations of the epidermal growth factor receptor gene predict prolonged survival after gefitinib treatment in patients with non-small-cell lung cancer with postoperative recurrence. J Clin Oncol 2005;23:2513-20.
16. Takano T, Ohe Y, Sakamoto H, et al. Epidermal growth factor receptor gene mutations and increased copy numbers predict gefitinib sensitivity in patients with recurrent non-small-cell lung cancer. J Clin Oncol 2005;23:6829-37.
17. Tsao MS, Sakurada A, Cutz JC, et al. Erlotinib in lung cancer—molecular and clinical predictors of outcome. N Engl J Med 2005;353:133-44.
18. Leon SA, Shapiro B, Sklaroff DM, Yaros MJ. Free DNA in the serum of cancer patients and the effect of therapy. Cancer Res 1977;37:646-50.
19. Sasaki H, Endo K, Konishi A, et al. EGFR Mutation status in Japanese lung cancer patients: genotyping analysis using LightCycler. Clin Cancer Res 2005;11: 2924-9.
20. Marchetti A, Martella C, Felicioni L, et al. EGFR mutations in non-small-cell lung cancer: analysis of a large series of cases and development of a rapid and sensitive method for diagnostic screening with potential implications on pharmacologic treatment. J Clin Oncol 2005;23:857-65.
21. Kobayashi S, Boggon TJ, Dayaram T, et al. EGFR mutation and resistance of non-small-cell lung cancer to gefitinib. N Engl J Med 2005;352:786-92.
22. Kwak EL, Sordella R, Bell DW, et al. Irreversible inhibitors of the EGF receptor may circumvent acquired resistance to gefitinib. Proc Natl Acad Sci U S A 2005; 102:7665-70.
23. Pao W, Miller VA, Politi KA, et al. Acquired resistance of lung adenocarcinomas to gefitinib or erlotinib is associated with a second mutation in the EGFR kinase domain. PLoS Med 2005;2:e73.
24. Pao W, Wang TY, Riely GJ, et al. KRAS mutations and primary resistance of lung adenocarcinomas to gefitinib or erlotinib. PLoS Med 2005;2:e17.

EGFR Mutation of Tumor and Serum in Gefitinib-Treated Patients with Chemotherapy-Naive Non–small Cell Lung Cancer

Hideharu Kimura, MD, Kazuo Kasahara, MD, Kazuhiko Shibata, MD, Takashi Sone, MD, Akihiro Yoshimoto, MD, Toshiyuki Kita, MD, Yukari Ichikawa, MD, Yuko Waseda, MD, Kazuyoshi Watanabe, MD, Hiroki Shiarasaki, MD, Yoshihisa Ishiura, MD, Masayuki Mizuguchi, MD, Yasuto Nakatsumi, MD, Tatsuhiko Kashii, MD, Masashi Kobayashi, MD, Hideo Kunitoh, MD, Tomohide Tamura, MD, Kazuto Nishio, MD, Masaki Fujimura, MD, and Shinji Nakao, MD

Background: The authors evaluate the efficacy and safety of gefitinib monotherapy in chemotherapy-naive patients with advanced non–small-cell lung cancer (NSCLC). A secondary endpoint is to evaluate the relationship between clinical manifestations and epidermal growth factor receptor (*EGFR*) mutation status.

Methods: Japanese chemotherapy-naive NSCLC patients were enrolled. They had measurable lesions, Eastern Cooperative Oncology Group performance status of 0 to 2, and adequate organ and bone marrow function. Patients received 250 mg of oral gefitinib daily. *EGFR* mutations in exon 18, 19, and 21 of DNA extracted from tumor and serum were analyzed by genomic polymerase chain reaction and direct sequence.

Results: All 30 patients were eligible for the assessment of efficacy and safety. An objective response and stable disease were observed in 10 patients (33.3%) and nine patients (30.0%), respectively. The median time to progression was 3.3 months and the median overall survival was 10.6 months. The 1-year survival rate was 43.3%. Grade 3 toxicities were observed in seven patients. *EGFR* mutation was observed in four of 13 (30.8%) tumors, and two of them achieved partial response. In serum samples, three of 10 patients with *EGFR* mutations in the serum before treatment had a response to gefitinib. *EGFR* mutation was observed in 10 of 27 and significantly more frequently observed in the posttreatment samples from patients with a partial response or stable disease than in those from patients with progressive disease ($p = 0.006$).

Conclusions: Gefitinib monotherapy in chemotherapy-naive NSCLC patients was active, with acceptable toxicities. These results warrant further evaluation of gefitinib monotherapy as a first-line therapy. The *EGFR* mutation in serum DNA may be a biomarker for monitoring the response to gefitinib during treatment.

Key Words: Non–small-cell lung cancer, Gefitinib, Epidermal growth factor receptor, Mutation, Serum DNA.

(*J Thorac Oncol.* 2006;1: 260–267)

Non–small-cell lung cancer (NSCLC) is the leading cause of cancer death in Japan and throughout the world.[1] Unfortunately, the majority of patients with NSCLC present with locally advanced or metastatic disease at the time of diagnosis. Although chemotherapy has produced modest survival benefits in advanced NSCLC patients, the outcome of chemotherapy for NSCLC remains unsatisfactory.

Protein tyrosine kinases play important roles in the pathogenesis of malignant tumors.[2] Among them, epidermal growth factor receptor (EGFR) tyrosine kinase has been implicated in the initiation and progression of NSCLC.[3–5] The overexpression of EGFR is frequent in NSCLC.[6] Monoclonal antibodies and low-molecular-weight compounds that inhibit the EGFR signaling pathway have been developed and shown to have antitumor effects. Gefitinib (Iressa, AstraZenca, London, England) is an orally active EGFR type tyrosine kinase inhibitor. In four phase I studies, tumor shrinkage or stabilization after gefitinib monotherapy was observed in some patients with NSCLC. In two phase II trials, Iressa Dose Evaluation in Advanced Lung cancer (IDEAL) 1 and 2, gefitinib monotherapy was shown to have a substantial effect in NSCLC patients treated previously with chemotherapy.[7,8] In these trials, patients of Asian origin and who had never been smokers had a statistically significant improvement in overall survival. In spite of encouraging results in the IDEAL trials, two large-scale, phase III, randomized trials, Iressa NSCLC Trial Assessing Combination Treatment, failed to show any survival benefit for the use of gefitinib.[9,10] Patients in a large-scale phase III trial comparing gefitinib

From Respiratory Medicine, Kanazawa University Hospital, Ishikawa; Internal Medicine, Kouseiren Takaoka Hospital, Takaoka; Internal Medicine, Shinminato Municipal Hospital, Shinminato, Japan. Internal Medicine, Fukuiken Saiseikai Hospital; Respiratory Medicine, Toyama City Hospital, Toyama; Respiratory Medicine, Ishikawa Prefectoral Hospital, Kanazawa; Respiratory Medicine, Kanazawa Municipal Hospital; Kanazawa; and National Cancer Center Hospital, and National Cancer Center Research Institute, Tokyo, Japan.

Address for correspondence: Kazuo Kasahara, MD, Takara-machi 13-1, Kanazawa, Ishikawa, Japan; email: kasa1237@med3.m.kanazawa-u.ac.jp.

ISSN: 1556-0864/06/0103-0260

and placebo in advanced NSCLC with prior chemotherapy demonstrated in preliminary analysis a tendency to have improvement in overall survival but did not have a statistically significant improvement in overall survival.[11] There are many issues that need to be addressed with regard to the clinical application of gefitinib; one of the most important issues is the efficacy of gefitinib monotherapy in patients with chemotherapy-naive NSCLC,[12] and another is to establish a way to predict response to gefitinib.

Recently, it has been suggested that mutations in the EGFR tyrosine kinase domain play a critical role in determining tumor response to gefitinib in NSCLC patients.[13,14] The mutations consisted of small, in-frame deletions or substitutions clustered around the adenosine triphosphate–binding site in exons 18, 19, and 21 of the *EGFR*. After these reports, some investigators supported the belief that *EGFR* mutation is one of the strong determinants of tumor response to gefitinib.[15–17] Tumors with *EGFR* mutations tend to be more common in adenocarcinomas, female patients, nonsmokers, and those of Asian origin. In most of those studies, tumor samples that were resected by operations were used. Because it is often difficult to obtain a tumor sample from an inoperable NSCLC patient, it is necessary to establish a method for detecting mutant *EGFR* from a patient sample other than from tumor specimens.

Polymerase chain reaction (PCR) technology for the amplification of small amounts of DNA has made it possible to identify the same alterations typically observed in DNA from serum samples from NSCLC patients.[18,19] Serum DNA may provide a noninvasive and repeatable source of genotypic information that could influence treatment and prognosis, especially in advanced NSCLC patients who have received gefitinib therapy. We essentially consider that it is possible to detect the *EGFR* mutation in serum DNA. We hypothesized that serum DNA may provide useful information on *EGFR* mutations in lung cancer patients.

As described above, the usefulness of gefitinib monotherapy is controversial and that in patients without pretreatment is unclear. Because *EGFR* mutations have been shown to be strongly associated with the response of NSCLC patients to gefitinib treatment, the analysis of *EGFR* mutations is necessary to evaluate the clinical benefit of gefitinib. We therefore conducted a multicenter phase II trial for these patients. The primary objective was to evaluate the objective response rate, and secondary objectives were to estimate the disease control rate, disease-related symptom improvement rate, safety, time to progression (TTP), and overall survival (OS). In addition, as a correlative study, we planned to detect *EGFR* mutations in serum samples from NSCLC patients and evaluate the relationship between the *EGFR* mutation and clinical manifestations in NSCLC patients receiving gefitinib treatment.

PATIENTS AND METHODS

Patient Eligibility

Patients who had histologically or cytologically proven stage IIIb or IV NSCLC and no previous chemotherapy were enrolled into this trial. Radiotherapy for metastatic lesions until 3 weeks before entry was allowed on condition that these lesions were not assessed for tumor response. Patients in whom recurrence occurred after surgery were also eligible. Patient eligibility criteria included at least one measurable lesion, age of 20 years or older, Eastern Cooperative Oncology Group performance status (PS) of 0 to 2, and life expectancy of greater than or equal to12 weeks. Adequate organ and bone marrow function was necessary, defined as leukocyte counts greater than or equal to 3.0×10^6/liter, neutrophil counts greater than or equal to 1.5×10^6/liter, platelet counts greater than or equal to 100×10^9/liter, hemoglobin levels greater than or equal to 8.5 g/dl, alanine aminotransferase or aspartate aminotransferase levels less than or equal to two times the upper limit of the reference range (<100 IU/liter in the presence of liver metastases), serum bilirubin levels less than or equal to 1.5 mg/dl, serum creatinine levels less than or equal to1.5 mg/dl, and PaO_2 levels greater than or equal to 65 mmHg. Patients with any of the following were excluded: active double cancer; severe complications such as myocardial infarction within 3 months before entry or uncontrolled diabetes; symptomatic brain or bone metastasis; diarrhea more severe than grade 2 according to National Cancer Institute Common Toxicity Criteria version 2; systemic administration of steroids to treat skin diseases; pleural, pericardial, or peritoneal effusion requiring treatment; and pregnancy or lactation. All patients were required to give informed consent.

Treatment

Patients were treated with gefitinib 250 mg orally once per day. Treatment was discontinued when the disease progressed, intolerable toxicities appeared, the patients requested withdrawal, or disease-related symptoms worsened without tumor response after 8 weeks of gefitinib monotherapy. These patients received chemotherapeutic treatment after gefitinib therapy. The chemotherapy regimen consisted of platinum (cisplatin or carboplatin) plus new agents (paclitaxel, docetaxel, gemcitabine, vinorelbine, or irinotecan) in patients aged 74 years or younger and vinorelbine monotherapy in patients aged 75 years or older. If symptomatic bone or brain metastasis occurred during gefitinib monotherapy, patients received radiotherapy after gefitinib treatment.

Efficacy and Drug-Related Adverse Events

Tumor size was assessed with computed tomography or magnetic resonance imaging scans every 4 weeks from the start to cessation of protocol treatment, using Response Evaluation Criteria in Solid Tumors guidelines.[20] Disease control was judged when patients achieved the best response of complete response, partial response (PR), or stable disease (SD), which was confirmed and sustained for 4 weeks. TTP was measured as the period from the start of the treatment to an identifiable time of disease progression. OS was measured from the start of the treatment until death or the last follow-up. The Kaplan-Meier method was used to calculate these measures.

Drug adverse events were recorded and graded according to National Cancer Institute Common Toxicity Criteria version 2.0. Changes in physical and laboratory findings were assessed at least every 2 weeks.

Serum Sample Collection and DNA Extraction

Blood samples from patients were collected before and 14 days after the initiation of gefitinib administration. Separated serum was stocked at −80°C until use. DNA extraction from the serum samples was performed using a nonorganic method (Oncor, Gaithersburg, MD). Serum DNA was purified using Qiamp Blood Kit (Qiagen, Hilden, Germany), with the following protocol modifications. One column was used repeatedly until the whole sample had been processed. The extracted DNA was stocked at −20°C until use.

Tissue Sample Collection and DNA Extraction

Tumor specimens were obtained on protocols approved by the institutional review board. Twenty paraffin blocks of tumor material, obtained from 15 patients for diagnosis before treatment, were collected retrospectively. Eleven tumor samples were collected from primary cancer by means of transbronchial lung biopsy, one was resected by operation, and nine were from metastatic sites (four from bone, three from lymph nodes, one from the brain, and one from the colon). All specimens underwent histologic examination to confirm the diagnosis of NSCLC. DNA extraction from tumor samples was performed using the TaKaRa DEXPAT kit (TaKaRa Biomedicals, Shiga, Japan).

PCR Amplification

PCR was performed in 25-μl volumes using 15 μl of template DNA, 0.75 units of Ampli Taq Gold DNA polymerase (Perkin-Elmer, Roche Molecular Systems, Inc., Branchburg, NJ), 2.5 μl of PCR buffer, 0.8 mM dNTP, 0.5 μM of each primer, and different concentrations of $MgCl_2$, depending on the polymorphic marker. A set of designed primers was used to amplify exon 19 of *EGFR* (upper primer, 5′-CAGCCCCCAGCAATATCAGCCTTAGGT-3′; lower primer, 5′- CACTAGAGCTAGAAAGGGAAAGACATA-3′). Thirty cycles of amplification were performed using a thermal cycler (Perkin-Elmer, Foster City, CA) (95°C for 45 seconds, 55.5°C for 30 seconds, 72°C for 30 seconds, followed by incubation at 72°C for 10 minutes). The bands were visualized using a 2100 bioanalyzer, DNA 500 Labchip kit (Aglient Technologies, Waldbronn, Germany). If no PCR products were detected by the first PCR, an additional 20 cycles of PCR was carried out and the sample was revisualized. To confirm the deletional mutation in exon 19, and to detect the mutation in exons 18 and 21 of *EGFR*, PCR was performed again using another primer set as described previously.[13]

Sequencing

Amplification and sequencing were performed in duplicate for each sample using an ABI prism 310 (Applied Biosystems). The sequences were compared with the GenBank-archived human sequence for *EGFR* (accession no. AY588246).

Trial Design and Statistical Methods

The trial was a two-stage multicenter phase II study. The primary endpoint was response rate, and secondary endpoints were disease control rate, safety, TTP, and OS. As a correlative study, *EGFR* mutations in tumor and serum samples were analyzed. The protocol and consent form were approved by the institutional review board of each participating hospital. Initially, 15 patients were recruited to the study. If one of these patients responded to treatment with gefitinib monotherapy, an additional 10 patients were recruited. If five or more of these 25 patients responded to therapy, treatment with gefitinib was concluded to be effective. According to Simon's minimax design,[21] our study, with a sample size of 25, had an 80% power to support the hypothesis that the true objective response rate was greater than 30% and a 5% significance to deny the hypothesis that the true objective response rate was less than 10%. Assuming a nonevaluability rate of less than 20%, we projected an accrual of 30 patients. In analysis of *EGFR* mutation in serum samples, the categorical variables were compared using the Fisher's exact test. A value of $p < 0.05$ was considered significant. The statistical analyses were performed using the StatView software package, version 5.0 (SAS Institute, Inc., Cary, NC).

RESULTS

Patients

From October of 2002 to August of 2003, 30 patients were enrolled into the study. Patient characteristics are summarized in Table 1. The most common histologic subtype was adenocarcinoma (25 patients [83.3%]). Three patients had undergone surgery and three had received radiotherapy to bone or brain metastases. Twenty patients were current or previous smokers. Twenty-six patients (86.7%) had good PS (0–1) and 86.7% of enrolled patients had stage IV disease. A total of 43 sites of metastatic lesions in 26 patients were diagnosed. Thirteen of the 26 patients had more than one metastatic lesion. All four patients with stage IIIb disease had pleural effusion and were ineligible for radiotherapy.

Efficacy

All patients were assessable for tumor response (Table 2). Complete response was not observed. Ten patients achieved PR, nine had SD as their best response, and 11 patients had progressive disease (PD). The objective response rate was 33.3% (95% confidence interval, 16.2–49.8%) and the disease control rate was 63.3% (95% confidence interval, 46.0–80.5%). All responders had adenocarcinoma. Of the responders, four were male patients and six were female patients. None of the prognostic factors such as gender (male versus female), PS (0–1 versus 2), smoking (never-smoker versus smoker), histology (adenocarcinoma versus nonadenocarcinoma), clinical stage (IIIb versus IV), and prior treatment (yes versus no) was significantly associated with tumor responses (Table 2). Disease control was observed in 19 patients (eight men and 11 women). A significantly higher disease control rate was observed in female patients (p = 0.018) and nonsmokers (p = 0.049). The other factors did not affect the disease control rate (Table 2).